ANL-IFR-91

Integral Fast Reactor
Integral Fast Reactor
Integral Fast Reactor
Integral Fast Reactor
Integral Fast Reactor
Integral Fast Reactor
Integral Fast Reactor
Integral Fast Reactor
Integral Fast Reactor
Integral Fast Reactor
Integral Fast Reactor
Integral Fast Reactor
Integral Fast Reactor
Integral Fast Reactor
Integral Fast Reactor
Integral Fast Reactor
Integral Fast Reactor
Integral Fast Reactor
Integral Fast Reactor
Integral Fast Reactor
Integral Fast Reactor
Integral Fast Reactor
Integral Fast Reactor
Integral Fast Reactor
Integral Fast Reactor
Integral Fast Reactor
Integral Fast Reactor
Integral Fast Reactor
Integral Fast Reactor
Integral Fast Reactor
Integral Fast Reactor
Integral Fast Reactor

IFR

Reactor Material Debris Formation Scoping Tests

by J. D. Gabor, R. T. Purviance, R. W. Aeschlimann, and B. W. Spencer

Argonne National Laboratory, Argonne, Illinois 60439
operated by The University of Chicago
for the United States Department of Energy under Contract W-31-109-Eng-38

IFR Technical Memorandum

Results reported in the IFR-TM series of memoranda frequently are preliminary and subject to revision. Consequently they should not be quoted or referenced.

DISCLAIMER

August 1988 ANL-IFR-91

REACTOR MATERIAL DEBRIS FORMATION SCOPING TESTS

by

J. D. Gabor, R. T. Purviance, R. W. Aeschlimann, and B. W. Spencer

Reactor Analysis and Safety Division
Argonne National Laboratory
9700 South Cass Avenue
Argonne, Illinois 60439

IFR TECHNICAL MEMORANDUM NO. 91

Results reported in the IFR-TM series of memoranda frequently are preliminary and subject to revision. Consequently they should not be quoted or referenced.

TABLE OF CONTENTS

LIST OF FIGURES

LIST OF TABLES

REACTOR MATERIAL DEBRIS FORMATION SCOPING TESTS

by

J. D. Gabor, R. T. Purviance, R. W. Aeschlimann, and B. W. Spencer

ABSTRACT

Although the Integral Fast Reactor (IFR) possesses inherent safety features, an assessment of the consequences of the melting of the metal fuel and its subsequent contact with sodium is necessary for risk analysis. A test series has therefore been conducted to study the breakup behavior of uranium alloy during downward relocation through sodium. In the previously reported first phase of this study eight tests were conducted in which the parameters were i) melt superheat, ii) injection velocity, iii) pour stream diameter, and iv) melt material. The parameters of the second phase of this study (reported here) were i) sodium depth, ii) melt superheat and iii) uranium-iron eutectic. The sodium depth ranged from 0.15 to 0.9 m and the superheat was 400C for tests with uranium (mp 1133C) and 800C for tests with the U-10 wt% Fe (mp 725C) eutectic. A 25-mm thick base plate was installed in the sodium vessel in the tests with shallow sodium depths (0.15 and 0.3 m) to determine impingement heat flux.

The particles produced by the pour stream breakup were primarily in the form of sheets with filament formation. Because the higher superheat for the U-10 wt% Fe tests permitted more hydrodynamic action before freezing, these particles were somewhat rounder and smaller (mean size ~4 mm) than the uranium particles (mean size ~10 mm). The particle shape could also be characteristic of the iron alloy. A sodium depth of less than 0.3 m was required for hydrodynamic breakup and freezing of the uranium melt pour stream. The temperature response of the base plate for particle bed impingement in the tests with shallow sodium pools was in reasonable agreement with a simple model based on semi-infinite mediums and average properties for the particle bed.

I. INTRODUCTION

The Integral Fast Reactor (IFR) is designed to have inherent safety features. An important feature is its pool configuration which facilitates passive decay heat removal and isolates the core from accidents that might occur elsewhere in the plant. The core is designed for inherent shutdown capability, and the uranium alloy fuel has superior heat transfer properties compared to oxide fuels. Although the IFR possesses these inherent safety features, an assessment of the consequences of the melting of the metal fuel and its subsequent contact with sodium is necessary for risk analysis.

The breakup of jets and drops of molten metals in various liquids other than uranium alloys in sodium have been studied by numerous investigators.[1-9] The studies have generally been on a gram scale except for aluminum and mixed oxides produced by thermite reactors. A program was therefore initiated to study the interaction of kilogram quantities of uranium alloy reactor materials in sodium. A series of eight Fuel Fragmentation Characterization tests (FFC series) was conducted in which the breakup behavior of uranium-zirconium alloy pour streams in sodium was studied.[10] The parameters investigated were:

i)	Melt superheat:	10, <u>100</u>, 300C
ii)	Sodium temperature:	<u>600</u>C
iii)	Injection velocity:	<u>2</u>, 10 m/s
iv)	Injector diameter:	12.5, <u>25</u> mm
v)	Cover gas:	<u>argon</u>
vi)	Fuel quantity:	<u>3</u> kg
vii)	Alloy composition:	U, <u>U-5 wt% Zr</u>, U-10 wt% Zr
viii)	Sodium depth:	<u>1.2</u> m

The base case for reference purposes is indicated by the underlined parameters.

The following conclusions were derived from this initial test series:

1. There were no vapor explosions from the mixing of kilogram quantities of molten uranium alloy and sodium in these tests. The interactions were benign as anticipated because the conditions of the pour stream and sodium were far from satisfying vapor explosion criteria.

2. In general the fragments were in the form of filaments and sheets with a mean particle size typically 10 mm and a high bed voidage in the order of 0.9.

3. Thermal equilibrium between the pour stream and sodium occurred in 2 to 3 seconds. This rapid achievement of thermal equilibrium is reflective of the high thermal conductivity of the uranium metal alloy and sodium.

4. In two tests with a low melt temperature (U at 1232C and U-5 wt% Zr at 1256C) compared to the base condition of 1346C, portions of the melt stream froze in a columnar shape before hydrodynamic breakup.

5. Particle size decreased with increased duration of the hydrodynamic action on the pour stream before freezing.

6. In the test with the high injection velocity of 10 m/s, the pour stream was dispersed into smaller fragments and a lower voidage bed than the low velocity tests in which the jet was accelerated by gravity to about 2 m/s.

7. Calculations based on typical bed conditions indicated that the debris from a meltdown of a metal fuel pool reactor would be largely coolable by conduction; and even if very deep debris beds were to form, boiling heat transfer would likely preclude further melt penetration.

The second phase of this test series is described in this report. The goals of the second phase test series entitled FDE for Fuel Drop Experiments were to obtain data on pour stream breakup lengths, impingement heat flux and behavior of U-10 wt% Fe eutectic. In this series, tests were conducted with the sodium pool depths ranging from 0.15 to 0.9 m. The pool depth for the FFC series was 1.2 m. These reduced depths gave additional information on pour stream breakup, solidification, and impingement heat transfer. A 25-mm thick base plate was installed in the interaction vessel for the shallow pool (0.15 and 0.3 m) tests in order to determine the temperature response of horizontal surfaces heated by contact with the pour stream material. Tests were also conducted with the low melting (725C) U-10 wt% Fe eutectic. The U-10 wt% Fe is a worst case consideration for the combination of molten uranium and structural steel.

II. EXPERIMENTAL

A. Facility and Apparatus

The experimental facility consisted of a concrete cell containing the Interaction Assembly and sodium transfer system and power supplies (induction generator for melting the fuel metals and variacs for sodium transfer), instrumentation and controls, and services. The basic layout for the main components of the facility is sketched in Fig. 1.

The Interaction Assembly is shown in Fig. 2. The assembly essentially consisted of a furnace/injection for melting the pour stream metals, an interaction vessel containing sodium and an overall containment vessel. The uranium metal alloys were melted inductively with a 30-kW 10,000-Hz TOCCO motor generator. A ZrO plug was removed pneumatically from a MgO crucible to initiate the downward pour of the fuel melt. The sodium was contained in 192-mm (7 9/16-in) ID interaction vessels of variable length. The interaction vessels were inserted into an interior liner constructed from Schedule 40 8-in. (7.981-in or 207.72-mm ID) stainless steel pipe which was heated by an array of ceramic heaters. The instrumentation for indicating conditions in the interaction vessel included a bundle of thermocouples spaced 152 mm apart in the sodium, sodium level indicators of the spark plug type, and a pressure transducer. For tests with shallow sodium pools in which impingement heat transfer occurred on a 25-mm thick base plate, three thermocouples were

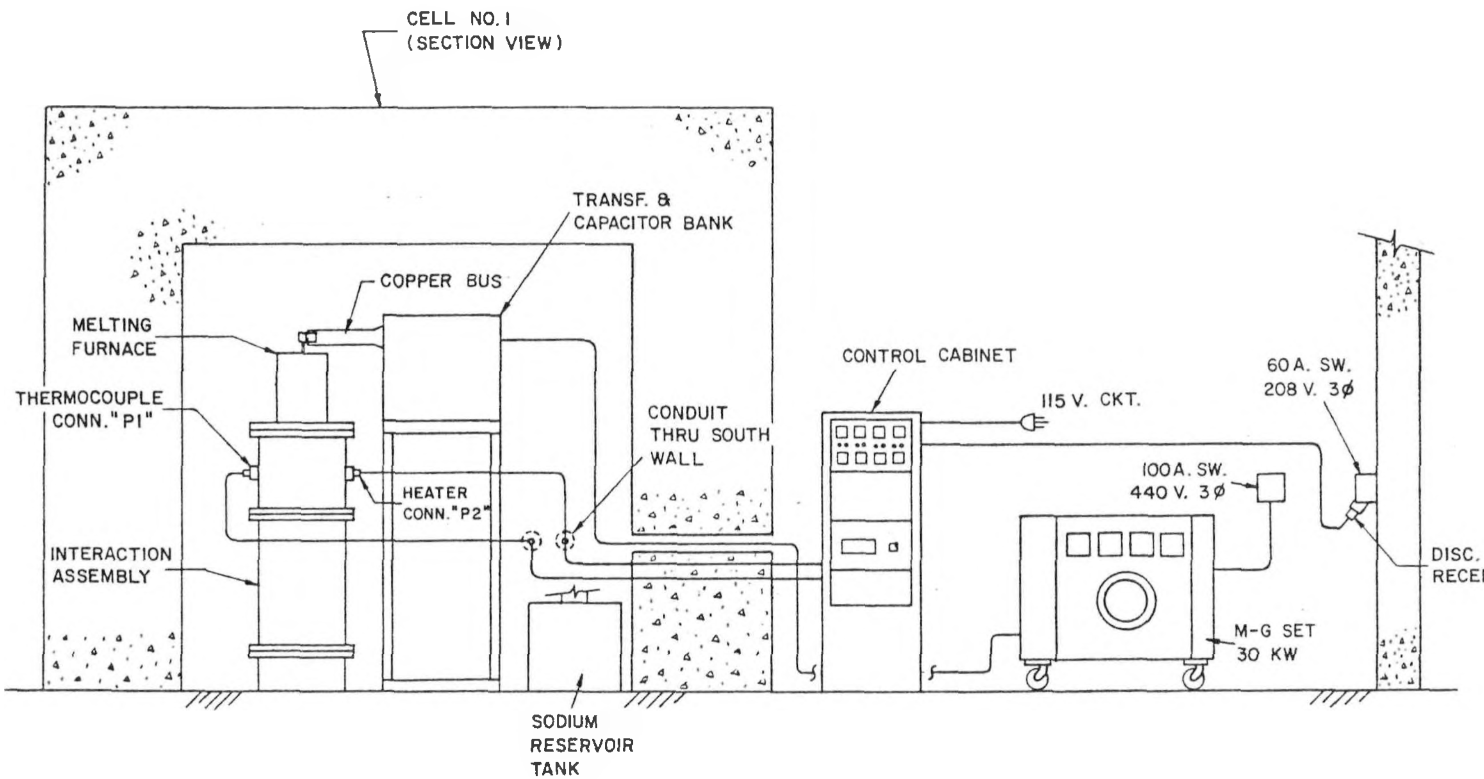

Fig. 1. Experimental Facility

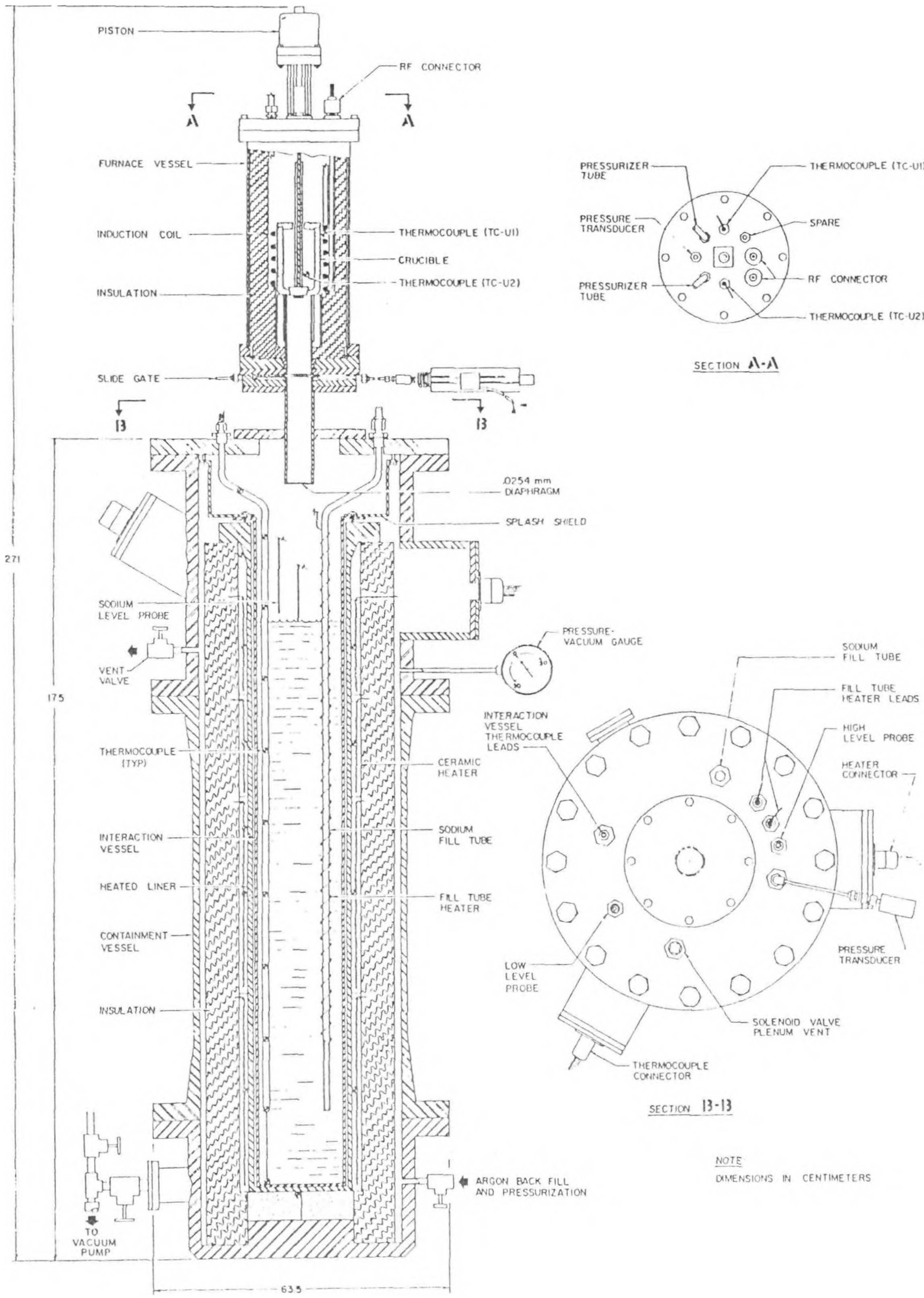

Fig. 2. Apparatus for Pour Stream Breakup Experiments

located in the center of the plate. The thermocouples were spaced at intervals of 6.4 mm from the sodium surface.

The thermocouple readings were recorded by a Digitrend Model 210 during the heatup phase. A Honeywell 1858 Visicorder and a Honeywell 101 magnetic tape unit were used to record thermocouple and pressure transducer data for the uranium alloy drop, Simpson type VoH-Ohmist meters determined electrical continuity created by sodium contact with the spark plug level indicators. Pairs of thermocouples were spot welded on opposite sides in the center of each ceramic heater section along the internal liner containing the interaction vessels. The heat was regulated by 0-1000C Weather Measure Model TPC-1 temperature controllers. An automatic test sequencer activated the plug removal, gate opening, solenoid valve closing, heater shut off and instrumentation in the fuel alloy injection sequence associated with the furnace/injector.

The facilities and apparatus are described in detail in the report on the Phase One series of drop tests.[10]

B. Test Parameters

The experimental conditions for both the Phase One (FDC series) and the current Phase Two (FDE series) test series are given in Table I. The melt superheat is based on the liquidus temperatures of the U-5 wt% Zr (1246C) and the U-10 wt% Zr (1360C), the U melting point (1133C) and the melting point of the U-10 wt% Fe eutectic (725C). The test with tin (mp 232C) was an initial proof test. The first four tests in the second phase (FDE series) described in this report were conducted with uranium at 400C superheat (1533C) and sodium depths decreasing from 0.9 to 0.15 m. A 25-mm thick base plate in the interaction vessel was used in the tests with a 0.15 and 0.3-m sodium depth for determination of impingement heat flux. The theoretical breakup length for this system ranges from 0.11 m by the Epstein and Fauske[13] model to the Taylor's[14] model 0.58-m length (see Appendix B). Without breakup of the pour stream, melt impingement on the base plate would occur.

Table I. Parameters for Pour Stream Breakup Experiments

Test	Melt Material	Melt[a] Superheat, °C	Sodium Temp, °C	Injection Velocity, m/s	Injection Diameter, mm	Melt Wt, kg	Sodium Depth, m	Comments
FFC-1[b]	Sn	100	200	2	25	1.2	1.2	Proof test
FFC-2	U	100	600	2	25	3	1.2	Tests 2 and 3 study alloy effect
FFC-3	U-10Zr	100	600	2	25	3	1.2	
FFC-4	U-5Zr	100	600	2	25	3	1.2	Reference test
FFC-5	U-5Zr	10	600	2	25	3	1.2	Tests 5 and 6 study effect of melt superheat
FFC-6	U-5Zr	300	600	2	25	3	1.2	
FFC-7	U-5Zr	100	600	2	12.5	3	1.2	Injection dia. variation
FFC-8	U-5Zr	100	600	10	25	3	1.2	Injection vel. variation
FDE-1	U	400	600	2	25	3	0.9	Tests 9, 10, 11, and 12 study hydrodynamic breakup length and impingement heat flux
FDE-2	U	400	600	2	25	3	0.6	
FDE-3	U	400	600	2	25	3	0.3	
FDE-4	U	400	600	2	25	3	0.15	
FDE-5	U-10Fe	800	600	2	25	3	0.3	Tests 13 and 14 study behavior of low melting iron eutectic.
FDE-6	U-10Fe	800	600	2	25	3	0.9	

[a]Based on liquidus temperature of alloys.

[b]FFC series reported in Reference 10

Test FDE-5 and -6 were with U-10 wt% Fe alloy melt. The melt temperature was 1525C which was essentially the same as for the first four tests with uranium metal; however, because of the low eutectic temperature (725C) of the iron alloy, the superheat was 800C. Test FDE-5 with the 0.3-m sodium depth gave impingement information, and FDE-6 with the 0.9-m sodium depth was conducted to characterize the fragments produced by hydrodynamic breakup.

After each test the sodium was withdrawn through the sodium fill tube to a depth of 152 mm. After the remaining sodium froze, the interaction vessel was removed from the assembly and radiographed. The vessel was then heated to remelt the sodium for drainage from the particle bed. The sodium remaining on the particles was removed chemically by reacting with ethanol.

C. Test Description

The tests of the Phase Two series are described below. The purpose of these experiments was to determine the hydrodynamic breakup length of the pour stream by varying the sodium depths for uranium metal drops and to obtain information on jet impingement and heat transfer. The tests with the U-10 wt% Fe were particularly significant in determining melt attack on steel structures.

1. FDE-1

The first test in the Phase Two series was conducted with pure uranium heated 400C above its melting point of 1133C. A previous test with uranium (FFC-2) in which the superheat was 100C resulted in freezing of portions of the pour stream before hydrodynamic breakup occurred. The purpose of this investigation was to determine what was the hydrodynamic breakup length for this metal-metal system. The sodium depth was therefore decreased to 0.9 m from the 1.2 m used in the previous tests and progressively decreased in the subsequent tests in order to determine at what depth the pour stream would impinge on the base plate of the interaction vessel before breakup occurred.

The response of the thermocouples in the interaction vessel is shown on the figures in Appendix C. TC-17 was at the sodium-argon interface with the subsequently numbered thermocouples at 0.15-m intervals below the interface. TC-23 was at the bottom of the sodium vessel. After the uranium drop TC-17 experienced a rapid increase of 13C within 2 s. The other thermocouples likewise experienced a similar rapid temperature increase. The average sodium temperature as a function of time after injection is shown on Fig. 3. Also shown on Fig. 3 are the average temperature responses of tests FDE-2, -3, and -4. As would be expected from a simple energy balance, the increase in sodium temperature is greater with the smaller sodium volumes. Because of the greater thermal inertia relative to the heat losses, the deeper sodium pools sustain an equilibrium temperature for a longer period of time whereas the temperature of the shallow pools tends to drift downward. In approximately two seconds thermal equilibrium was achieved.

A radiograph of the particle bed frozen in place in the sodium at the bottom of the interaction vessel is shown in Fig. 4. The sodium had been previously syphoned down to a level of 0.15 m. It was estimated from this radiograph that the material settled to the bottom of the vessel with an approximately 0.9 void fraction. This high voidage, which was typical of the first series of tests previously reported, would permit a high degree of coolability by both conduction and convection of the sodium phase.

Photographs of representative material after removal with ethanol are given in Figs. 5. The size distributions of the particles obtained in this test series is given in Table II. The mean particle size was 8.6 mm for FDE-1. The particles are irregular in shape. The material to a considerable degree is in the form of filaments and sheets typical of hydrodynamic breakup of metallic pour streams.

2. FDE-2

FDE-2, the second test in the Phase Two series, was identical to FDE-1 except that the sodium depth was reduced to 0.6 m. This was accomplished by shortening the length of the interaction vessel and maintaining the same distance (0.35 m) between the sodium surface and the bottom of the drop tube. The pour stream underwent hydrodynamic breakup and freezing before reaching the bottom of the sodium vessel. The particles that were produced by

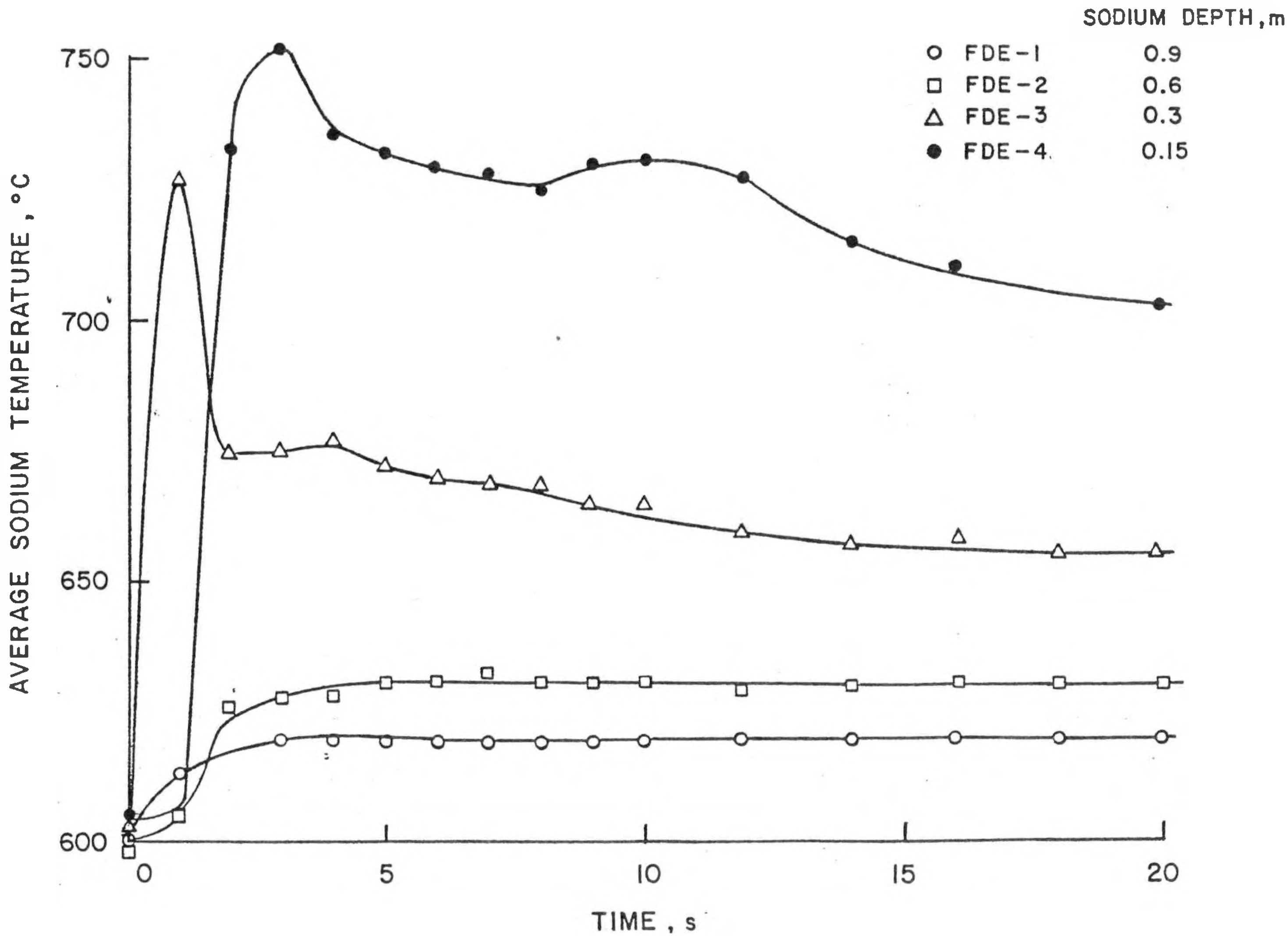

Fig. 3. Sodium Temperature Responses for FDE-1 to -4

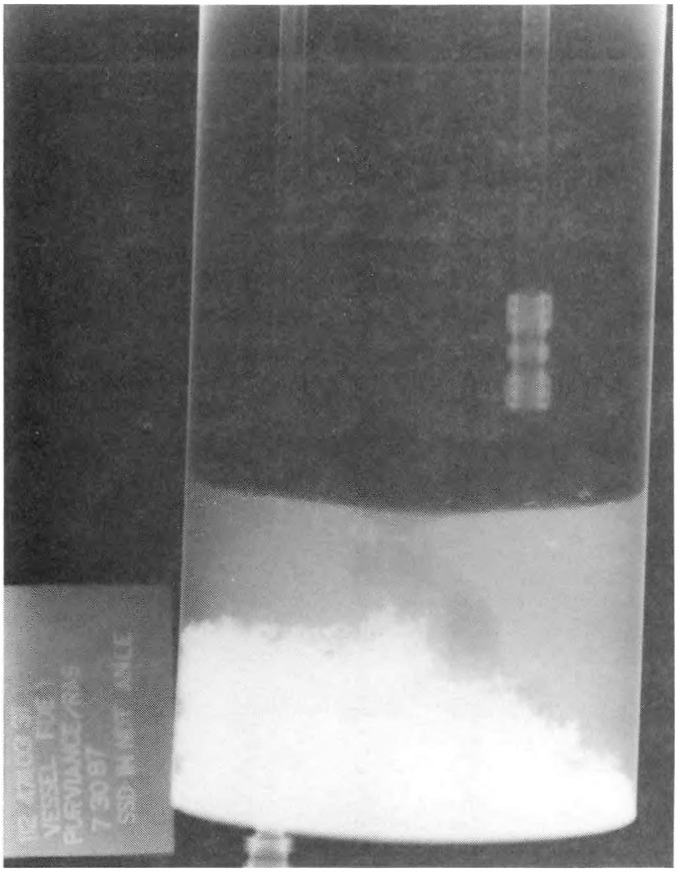

Fig. 4. Radiograph of Particle Bed for FDE-1

(a)

(b)

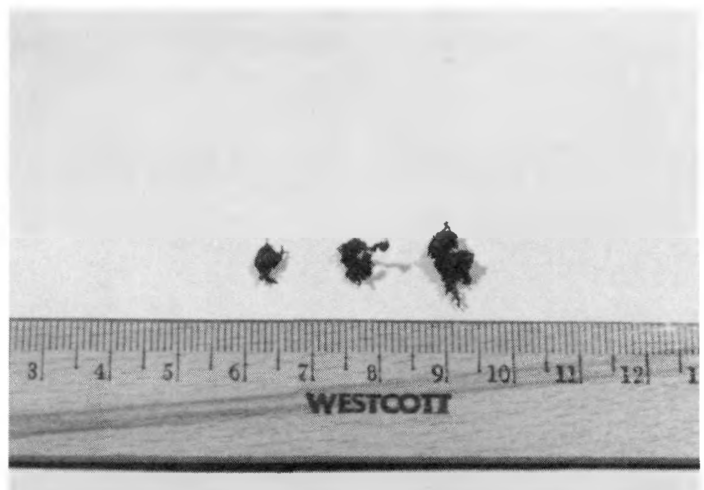

(c)

Fig. 5. Particles from FDE-1

Table II. Material Balances and Particle Bed Characteristics

Test No.	Charge, kg	Description of Material Recovered from Sodium				
		Size, mm	Weight, kg	Total Weight, kg	Bed Void Fraction	Mean Particle Size, mm[b]
FFC-2	2.983	70 to 150	1.790			
		10 to 45	0.480			
		5 to 20	0.280			
		< 0.1	0.006	2.556	0.95	16.13
FFC-3	2.989	25 to 65	0.358			
		10 to 40	0.437			
		5 to 25	1.661			
		< 0.1	0.006	2.462	0.95	9.68
FFC-4	3.007	40 to 110	1.610			
		15 to 30	0.348			
		1 to 15	0.351			
		< 0.1	0.007	2.316	0.95	10.54
FCC-5	3.000	70 to 300	1.829			
		10 to 50	0.412			
		5 to 25	0.291			
		< 0.1	0.007	2.539	0.97[a]	13.71
FCC-6	3.007	15 to 50	0.461			
		10 to 20	0.631			
		1 to 15	1.314			
		< 0.1 to 5	0.268	2.674	0.94	8.16
FCC-7	3.000	40 to 105	1.037			
		15 to 50	0.347			
		1 to 30	1.212			
		< 0.1	0.012	2.608	0.96	7.60
FCC-8	3.000	10 to 30	0.149			
		1 to 10	0.773			
		0.1 to 1	0.775			
		< 0.1	0.072	1.769	0.84	0.59
FDE-1	3.006	50 to 70	0.097			
		15 to 45	0.305			
		10 to 20	0.449			
		5 to 15	0.533			
		2 to 10	1.313	2.697	0.90	8.59
FDE-2	3.005	50 to 70	0.457			
		35 to 50	0.273			
		10 to 15	1.275			
		5 to 15	0.667	2.672	0.89	14.62
FDE-3	3.009	20 to 75	0.117			
		15 to 50	0.181			
		10 to 15	0.451			
		2 to 10	1.127			
		2 to 5	0.908	2.784	0.89	5.67
FDE-4	3.010	70 to 90	0.258			
		15 to 60	0.105			
		15 to 25	0.483			
		2 to 10	1.069	1.915	0.86	9.19[c]
		Agglomerate	~ 0.800			
FDE-5	2.998	2 to 5	0.188	0.188	0.76	3.5[c]
		Agglomerate	~ 2.600			
FDE-6	3.000	15 to 20	0.065			
		10 to 15	0.230			
		5 to 10	0.426			
		2 to 8	0.226			
		< 1 to 5	0.780	1.727	0.86	3.96

[a]Excludes frozen jet (70 to 300 mm portion).

[b]Mean diameter = $1/\sum^{i} [(\text{weight fraction})_i/dp_i]$

[c]Excludes agglomerated material

this interaction were therefore essentially the same as the first test FDE-1. Some typical particles are shown in Figs. 6. The particle bed again had a high voidage (0.9) and the mean particle size was 14.6 mm, somewhat higher than the 8.6-mm mean particle size of FDE-1. It is noted that the particle size was estimated by observation and not by any sizing technique such as sieving. The particles were highly irregular as can be seen in the accompanying photographs. It is not surprising that a good deal of deviation would occur in particle size distribution from run to run. It is felt that this run essentially repeats the first run and variations in particle size are representative of experimental deviation that can be expected from these tests.

3. FDE-3

FDE-3 was third in the sequence of tests with decreasing sodium depth. The sodium depth for this test was reduced to 0.3 m. For this test a 25-mm thick stainless steel base plate was installed in the sodium vessel to determine the temperature response of a horizontal surface as the hot pour stream material came in contact with it. The 0.3-m depth was observed to be sufficient for the pour stream to again hydrodynamically breakup and freeze before contacting the base plate of the sodium vessel. The particles were the same as shown in Figs. 5 and 6 for runs FDE-1 and -2. The mean particle size (5.7 mm) was somewhat smaller than the previous tests indicating good hydrodynamic breakup. The bed voidage (0.89) was in accord with the first two tests.

The temperature response of the base plate was measured with four thermocouples. TC-19 was at the base plate surface on the sodium side. TC-20, 21, and 22 were located 6, 12, and 18-mm in the base plate below the base plate-sodium interface. The responses of these thermocouples are combined in Fig. 7. The data were compared with a simple model for the temperature response following the contact of two semi-infinite media. It is seen that the rate of temperature decrease undergoes an arrest at ~2.5 s at 760C. The interface temperature upon contact of two semi-infinite media is determined by[11]

(a) (b)

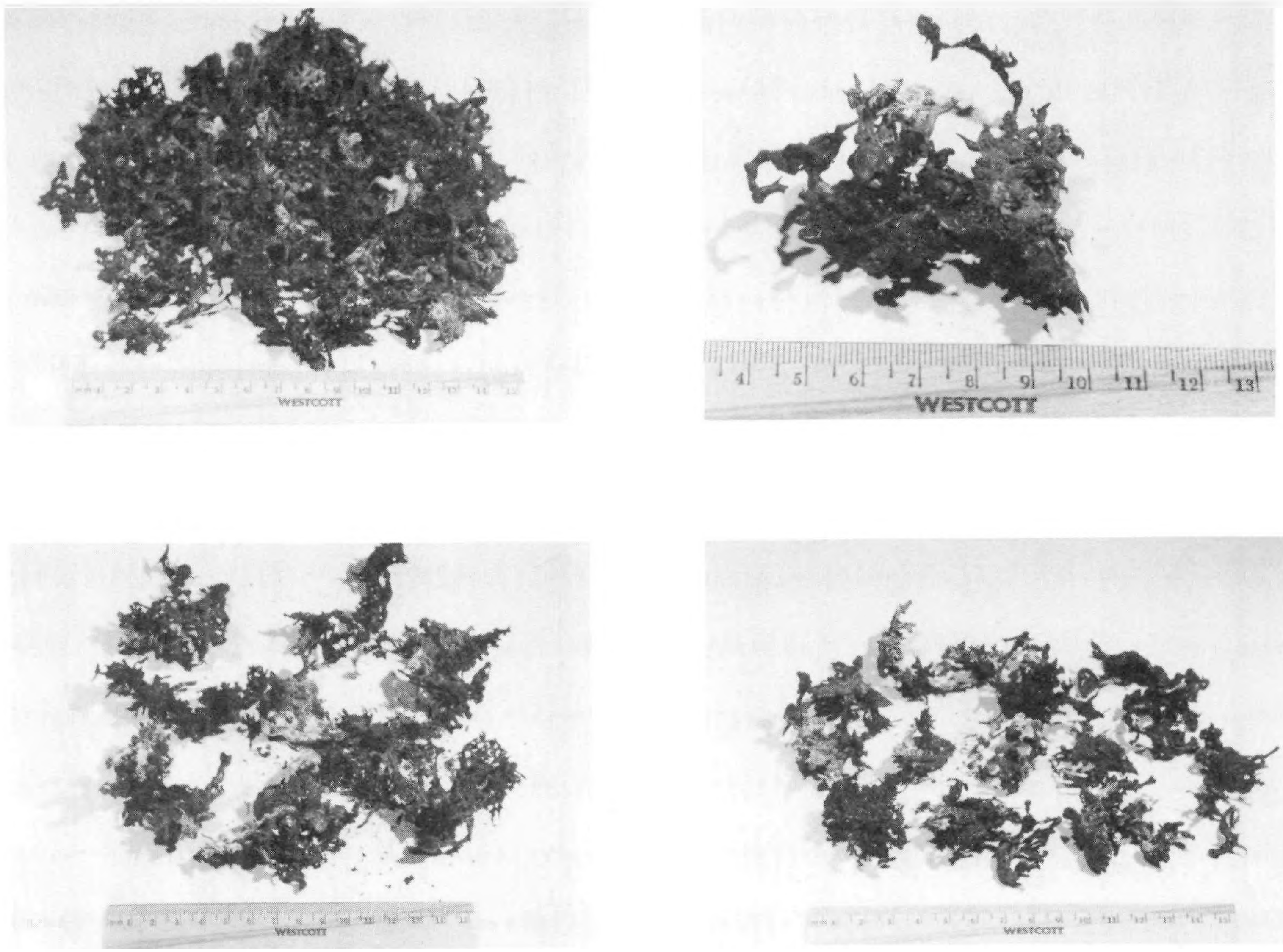

(c) (d)

Fig. 6. Particles from FDE-2

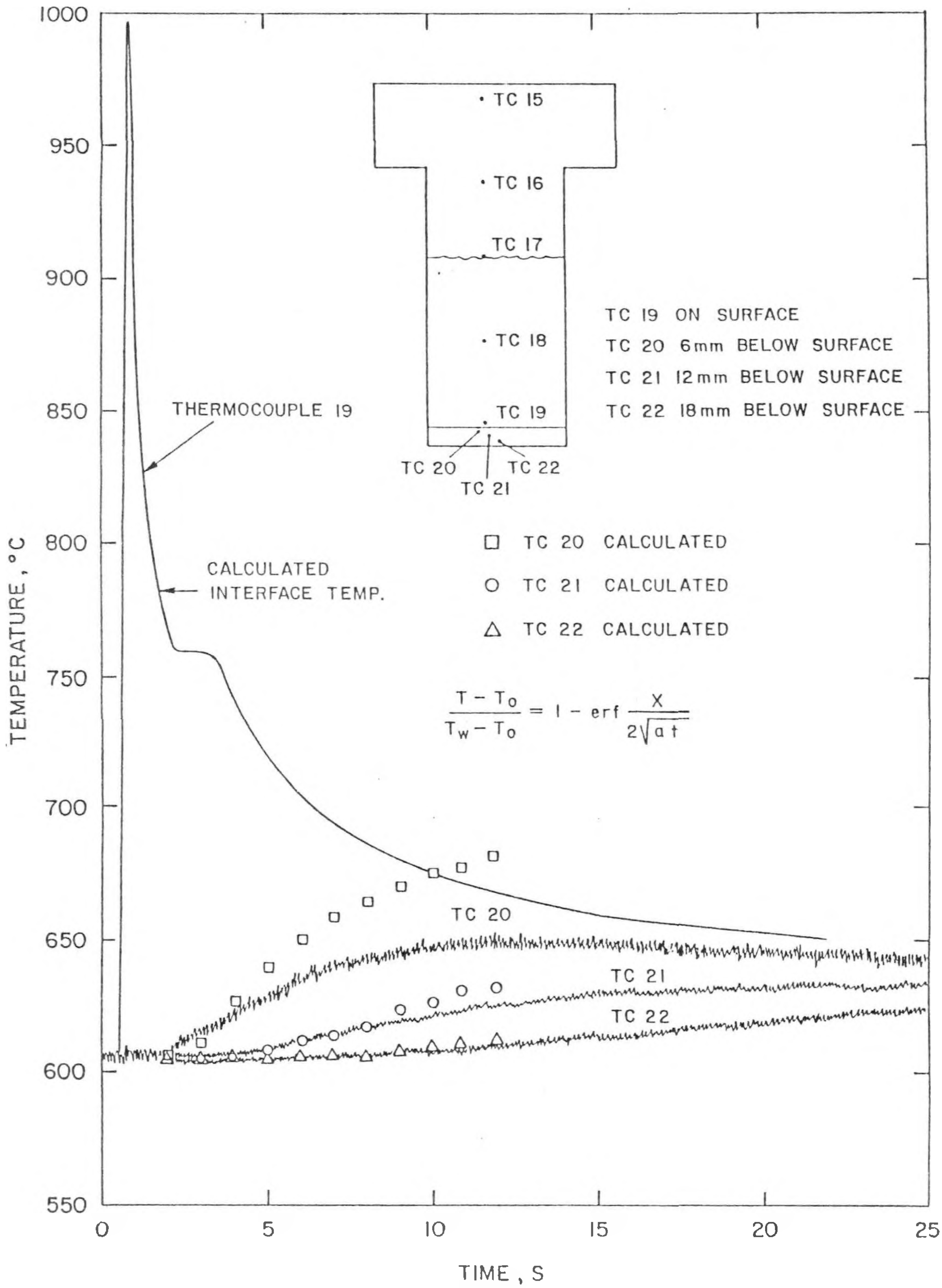

Fig. 7. Temperature Response of Base Plate for FDE-3

$$\frac{T_2 - T_i}{T_i - T_1} = \frac{K_1}{K_2}\sqrt{\frac{\alpha_2}{\alpha_1}} \qquad (1)$$

where

T_i = interface temperature
T_1 = initial temperature of steel
T_2 = initial temperature of uranium particle bed
K_1 = steel thermal conductivity
K_2 = particle bed effective thermal conductivity
α_1 = steel thermal diffusivity
α_2 = particle bed thermal diffusivity

For a uranium particle bed in sodium with a voidage of 0.89 the effective thermal conductivity is 54.8 W/mK. Taking the thermal conductivity of the steel phase to be 20.92 W/mK (see Appendix) and precontact temperatures of 1000C and 606C the calculated interface temperature is 782C (indicated by arrow on Fig. 7). The interface temperature was then used to calculate the subsequent rise of the steel base plate temperatures at the three thermocouple positions from the following equation[11]

$$\frac{T - T_1}{T_i - T_1} = 1 - \operatorname{erf}\frac{x}{2\sqrt{\alpha_1 t}}$$

where

T = temperature
T_1 = initial temperature of steel
T_i = interface temperature
x = distance coordinate
t = time
α_1 = steel thermal diffusivity

It is seen on Fig. 7 that the calculated temperature response of the steel base plate is in fairly good agreement with the measured response for about 5 s. The calculated temperatures eventually drift higher than the measured response for several reasons. One, of course, is that the physical system is not semi-infinite, and secondly, the calculation based on Eq. 2

assumes a constant interface temperature whereas actually the interface temperature as indicated by TC-19 declined. However, this simple model indicates that heat transfer from the particle bed to support structures is readily amenable to calculation.

4. FDE-4

For this test the sodium depth was further reduced to 0.15 m. Although there was evidence of extensive hydrodynamic breakup of the pour stream, the particles were not completely frozen when they reached the bottom. The particles sintered to form an agglomerate which did not adhere to the steel base plate (see Fig. 8). The voidage (0.86) of the mass of material was somewhat reduced compared to the previous tests but still very high indicating good coolability. The particles which did not agglomerate comprised about 70 percent of the drop material and had a mean particle size of 9.19 mm.

The behavior of the temperature response of the base plate was essentially the same as for FDE-3 in which the material was not sufficiently hot to sinter (see Appendix).

5. FDE-5

This test was conducted with U-10 wt% Fe at 1530C, which was at the same melt temperature as the first four tests. However, because U-10 wt% Fe is a eutectic with a low melting point of 725C, the pour stream initially was at 800C superheat compared to 400C for the first four tests. The alloy was formed by charging the MgO crucible with 2.7 kg of uranium and 0.3 kg of iron in the form of 6.3 mm balls. The sodium depth was 0.3 m for this tests. Approximately 93 percent of the particles formed from the pour stream breakup sintered to form an agglomerate before freezing. This agglomerate (Fig. 9) adhered to the 25-mm stainless steel base plate of the sodium vessel and could not be removed as in FDE-4. Apparently the higher superheat of the melt and the presence of iron resulted in melt attack on the stainless steel surface and bonding at freezing. The voidage estimated from the radiograph shown on Fig. 10 was still quite high at 0.76. Typical particles which did not sinter are shown in Fig. 11.

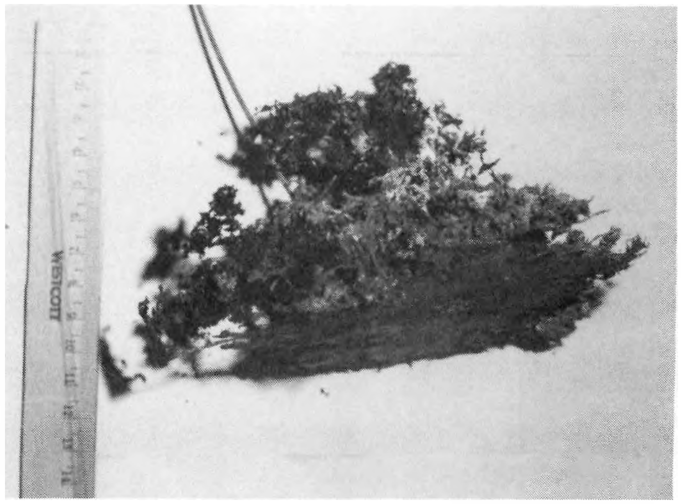

Fig. 8. Sintered Particle Agglomerate at Base of Sodium Vessel for FDE-4

Fig. 9. Sintered Particle Agglomerate at Base of Sodium Vessel for FDE-5

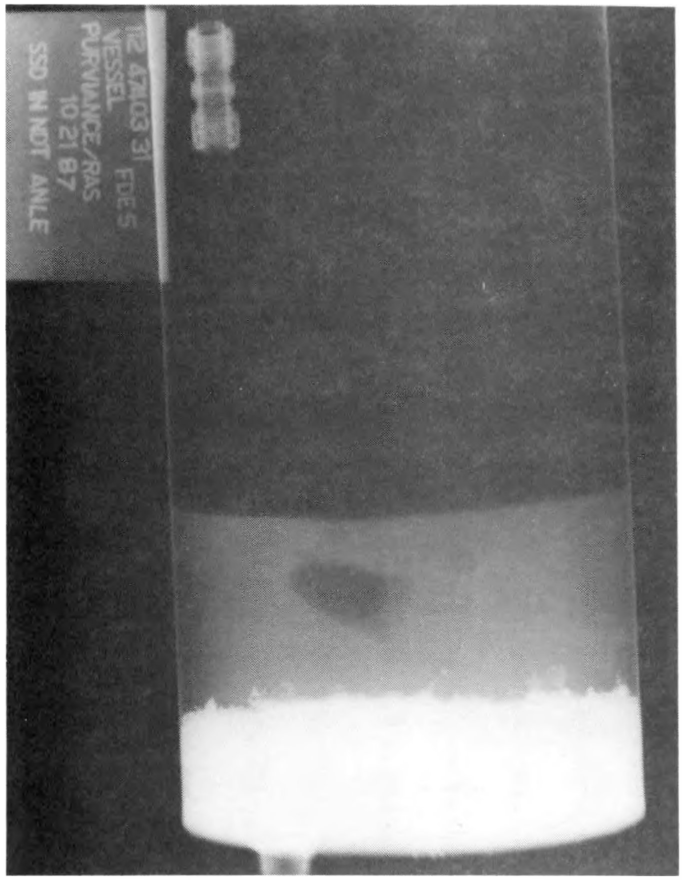

Fig. 10. Radiograph of Particle Bed for FDE-5

(a)

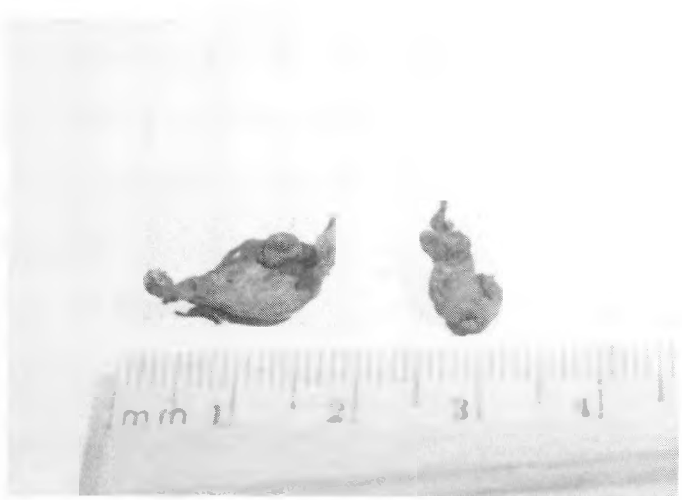

(b)

Fig. 11. Particles from FDE-5

The temperature responses of the sodium is shown on Fig. 12 for the two tests with U-10 wt% Fe. The responses are basically the same as for the uranium tests (Fig. 3). Equilibrium was achieved in about 2 s and because of the lower sodium mass in FDE-5 the increase in sodium temperature was greater than for FDE-6.

6. FDE-6

The purpose of this test was to characterize the particles produced by the hydrodynamic breakup of the U-10 wt% Fe pour stream. The sodium depth was increased to 0.9 m in order to extend the time for hydrodynamic breakup and freezing. During the melt heatup the MgO crucible cracked allowing about 1.3 kg of the alloy to leak out before discharge. The remaining 1.7 kg dropped into the sodium. It was felt that a sufficient amount of the melt had poured into the sodium to give a satisfactory characterization of the particles.

Representative particles are shown on Fig. 13. The particles tended to have their edges rounded with less evidence of filament formation. The particle shape may be a characteristic of the alloy material and the extended time for freezing because of the high superheat. The mean size was approximately 4 mm. This overall smaller particle size is attributed to the longer period for hydrodynamic breakup resulting from the higher superheat for this test. The bed voidage was again quite high at 0.86. The particles were not entirely solidified when they reached the base plate. A small agglomerate formed which adhered to the base plate (Fig. 14). It is of interest to again note that the agglomerates formed in the tests with the iron alloy fused into the steel base plate, whereas in Run 4 with pure uranium the particle agglomerate did not adhere. This may be indicative of the high potential for melt attack on steel structure with a uranium-iron alloy.

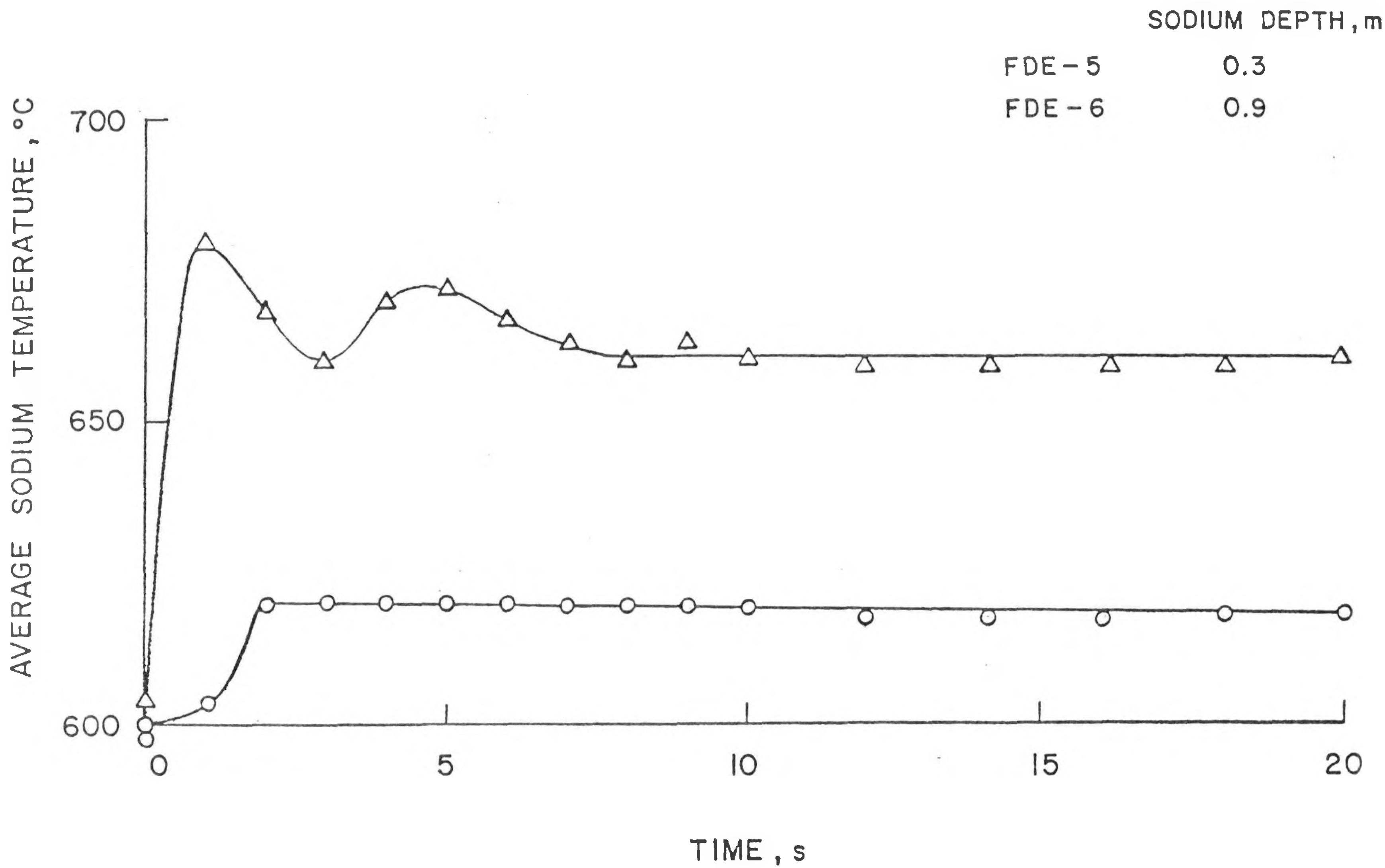

Fig. 12. Sodium Temperature Responses for FDE-5 and -6

(a)

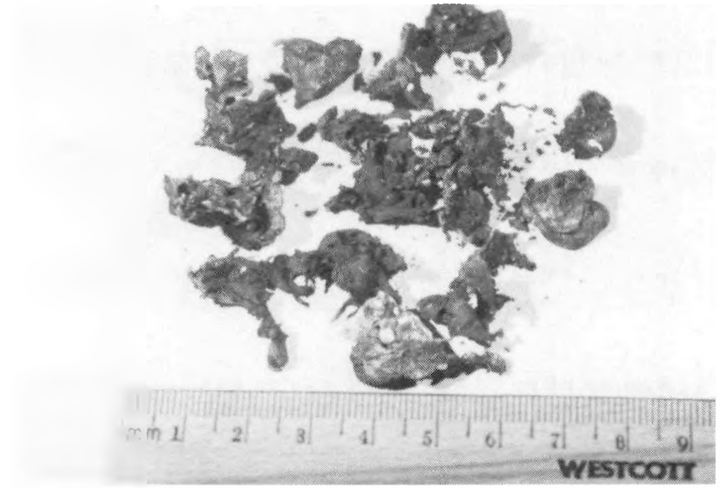

(b)

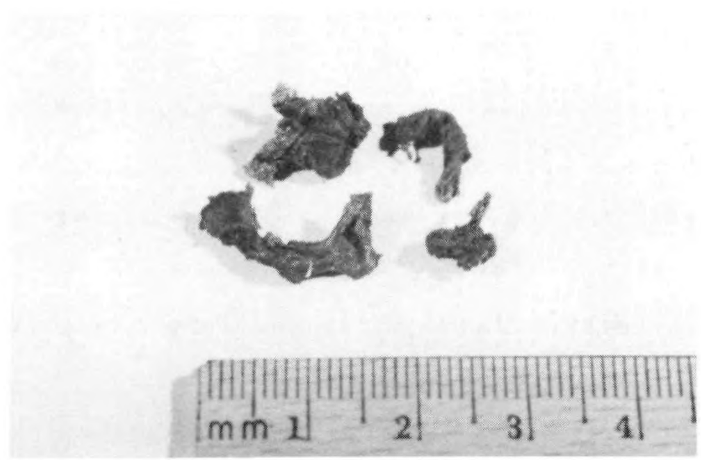

(c)

Fig. 13. Particles from FDE-6

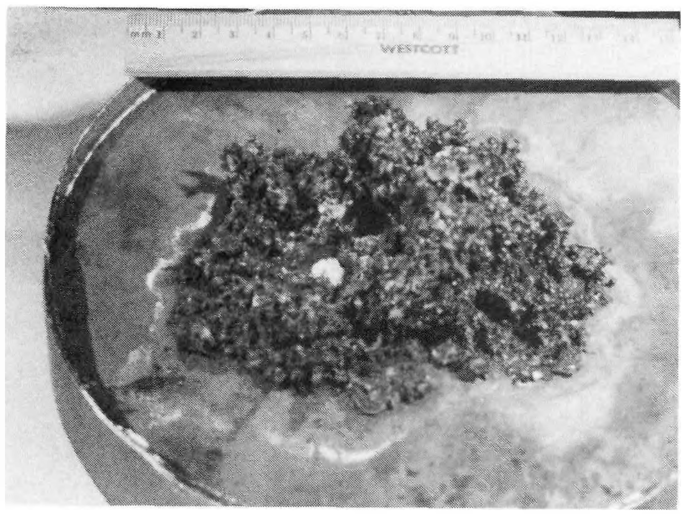

Fig. 14. Agglomerate Fused to Base Plate in FDE-6

III. CONCLUSIONS

1. The particles were primarily in the form of sheets with filament formation.

2. The U-10 wt% Fe particles were somewhat rounder and smaller (mean size ~4 mm) than the uranium particles (mean size ~10 mm) because the higher superheat for this uranium-iron alloy melt permitted more hydrodynamic action before freezing. The particle shape could also be characteristic of the iron alloy.

3. A sodium depth of less than 0.3 m was required for hydrodynamic breakup and freezing of the 25-mm diameter uranium pour stream.

4. The temperature response of the 25-mm steel base plate on impingement of the particle bed was in reasonable agreement with a simple model based on semi-infinite mediums and average properties for the particle bed.

5. The sintered agglomerate of uranium particles in FDE-4 did not adhere to the base plate while the U-10 wt% Fe alloy agglomerates in both tests FDE-5 and -6 fused into the base plate.

IV. REFERENCES

1. D. L. Swift and L. Baker, Jr., "Experimental Studies of the High-temperature Interaction of Fuel and Cladding Materials with Liquid Sodium," ANL-7120, Argonne National Laboratory (1965).

2. B. W. Spencer, L. M. McUmber, D. Gregorash, R. W. Aeschlimann, and J. J. Sienicki, "Corium Quench in Deep Pool Mixing Experiments," Trans. 23rd Natl Heat Trans. Conf., Denver, CO, August 1985.

3. B. W. Spencer, J. D. Gabor, J. C. Cassulo, and D. J. Kilsdonk, "Results of Scoping Experiments on Melt Stream Breakup and Quench," Proc. Intl. ANS/ENS Topical Mtg. on Thermal Reactor Safety, ANS 700106, San Diego, CA, Feb. 2-6, 1986.

4. K. Hartel and K. Martin, "Ein Rechenmodell zur Bestimmung der Hydrodynamischen Sätability von Flüssigketis-Freistrahlen in Flüssigkeit," KfK 3978, Kernforschungszentrum Karlsruhe (1986).

5. B. W. Spencer, J. D. Gabor, and J. C. Cassulo, "Effect of Boiling Regime on Melt Stream Breakup in Water," Proc. 4th Intl Symp. on Multi-Phase Transport and Particulate Phenomena, Miami Beach, FL, December 1986.

6. M. Berman, N. A. Evans, and M. S. Krein, "Core Melt/Coolant Interactions: Experiments," NUREG/CP-0048, Sandia National Laboratories, pp. 218-225, October 1983.

7. K. Miyazaki, K. Morimoto, O. Yamamoto, Y. Harada, and N. Yamoka, "Thermal Interaction of Water Droplet with Molten Tin," J. Nucl. Sci. Technol., 21, pp. 907-918 (1984).

8. J. D. Gabor, R. T. Purviance, R. W. Aeschlimann, and B. W. Spencer, "Characterization of IFR Metal Fuel Fragmentation," Trans. Am. Nucl. Soc., 54, pp. 251-253 (June 1987).

9. B. W. Spencer and J. F. Marchaterre, "Scoping Studies of Vapor Behavior during a Severe Accident in a Metal-Fueled Reactor," Proc. Intl. Topical Mtg. on Fast Reactor Safety, Knoxville, TN, CONF-850410, Vol. 1, p. 151, April 21-25, 1985.

10. J. D. Gabor, R. T. Purviance, R. W. Aeschlimann, and B. W. Spencer, "Characterization of Metal Fuel Fragmentation," ANL-IFR-52, August 1986.

11. W. M. Rohsenow, J. P. Hartnett, and E. N. Ganic, Eds., "Handbook of Heat Transfer Fundamentals," 2nd Ed., P. J. Schneider, "Conduction," Chap. 4, McGraw-Hill Book Company, N.Y., 1985.

12. M. Abramowitz and I. A. Stegun, Eds., "Handbook of Mathematical Functions with Formulas, Graphs, and Mathematical Tables," National Bureau of Standards Applied Mathematics Series, Fifth Printing, August 1966.

13. M. Epstein and H. K. Fauske, "Steam Film Instability and the Mixing of Core-melt Jets and Water," ANS Proc, 1985 Natl Heat Transfer Conf, ANS #700101, Denver, CO (August 1985).

14. G. I. Taylor, "The Dispersion of Jets of Metals at Low Melting Point in Water," The Scientific Papers of G. I. Taylor, Vol. III, ed. G. K. Batchelor (1940).

15. G. I. Taylor, "Generation of Ripples by Wind Blowing Over a Viscous Fluid," The Scientific Papers of G. I. Taylor, Vol. III, ed. G. K. Batchelor (1940).

16. V. C. Levich, "Physiochemical Hydrodynamics," Prentice-Hall, Inc., Englewood Cliffs, NJ (1962).

V. ACKNOWLEDGMENTS

This investigation was aided by many people. The assistance of B. T. Banez, J. C. Cassulo, R. M. Hodges, and R. H. Wesel in experimental operations is gratefully recognized. The preparation of the figures of J. Kawka is greatly appreciated. Thanks are owed to K. Rank, L. Pavlik and V. Eustace for the typing of this report.

APPENDIX A

CALCULATIONS OF TEMPERATURE RESPONSE OF BASE PLATE

The calculations are based on a two step process: 1) determination of the interface temperature on contact of the particle bed with the steel base plate and 2) determination of the interior temperature response of the steel base plate using the calculated interface temperature. These calculations were based on the simplifying assumption of two semi-infinite solids at uniform but different initial temperatures coming together in perfect contact. On this basis the mutual interface temperature immediately assumes a steady value of T_i.[11]

$$T_i = T_1 + \frac{T_2 - T_1}{1 + \sqrt{\rho_1 C_1 K_1 / \rho_2 C_2 K_2}} \qquad (1A)$$

where

T_i	=	interface temperature
T	=	initial temperature
C	=	heat capacity
K	=	thermal conductivity
ρ	=	density

and subscripts 1 and 2 refer to the steel and particle bed properties respectively. The properties used in these calculations are given in Table A1. The particle bed properties were estimated by weight averaging the volume fractions of the sodium and uranium phases.

$$\rho_2 C_2 K_2 = \varepsilon(\rho CK)_{Na} + (1 - \varepsilon)(\rho CK)_U \qquad (2A)$$

where ε is the volume fraction of sodium (Na) and $(1 - \varepsilon)$ is the volume fraction of uranium (U). The temperature response of the steel base is[11]

$$\frac{T - T_1}{T_i - T_1} = 1 - \text{erf}\ \frac{x}{2\sqrt{\alpha_1 t}} \qquad (3A)$$

where T refers to the steel temperature at position x at time t and α is the thermal diffusivity ($K/\rho C$). The experimental temperature responses were compared to the values determined from the above equations.

Table A1.
Properties Used in Temperature Response Calculations

Material	ρ, kg/m³	C, J/kgK	K, W/mK
Sodium	769.8	1.262×10^3	55.55
Uranium	17,500	0.161×10^3	54.7
Steel	7,600	0.6276×10^3	20.92

FDE-3

The base plate initial temperature was 606C before contact with the particles (see Fig. 7). The thermocouple (TC-19) located on the top surface of the base plate peaked at 1000C which was taken as the initial particle bed temperature. The subsequent decline in temperature was arrested for a period of 1.5 s at 760C which was taken as the experimental interface temperature. For this case with ε = 0.887 Eq. 2A gives

$$\rho_2 C_2 K_2 = (.887)(5.40 \times 10^7) + (.113)(1.54 \times 10^8) = 6.53 \times 10^7$$

Using this value for the particle bed the interface temperature can be calculated from Eq. 1A

$$T_i = 606 + \frac{1000 - 606}{1 + \sqrt{9.98 \times 10^7 / 6.53 \times 10^7}} = 782C$$

The calculated interface temperature of 782C is comparable to the 760C observed temperature arrest. The observed value of 760 will be used as the interface temperature in the temperature response calculation.

The steel temperature response can then be determined from Eq. 3A and compared with the responses of the thermocouples located 6.35, 12.7, and 19.05 mm below the surface. For steel

$$\alpha_1 = \frac{K_1}{\rho_1 C_1} = \frac{20.92}{(7600)(0.6276 \times 10^3)} = 4.39 \times 10^{-6} \ m^2/s$$

An example calculation is given below for the temperature at 6.35 mm below the surface at 5 s.[12]

$$\text{erf} \frac{x}{2\sqrt{\alpha t}} = \text{erf} \frac{6.35 \times 10^{-3}}{2\sqrt{(4.39 \times 10^{-6})(5)}} = 0.6638$$

Rearranging Eq. 3 to obtain T yields

$$T = T_1 + (T_i - T_1)\left[1 - \text{erf} \frac{x}{2\sqrt{\alpha t}}\right]$$

$$= 606 + (760 - 606)(1 - 0.6638)$$

$$= 658$$

If the calculated interface temperature of 782 were used, the calculated temperature for these conditions would be 665C. On the basis of the observed interface temperature of 760C response temperatures were tabulated on Table A2 and plotted on Fig. 7.

FDE-4

In this test with only a 0.15-m sodium depth the particles were not completely solidified when they reached the bottom and sintered to form an agglomerate. The observed interface temperature of 765C (Fig. A1) based on the arrest in temperature decline of the thermocouple on the base plate surface (TC-18) was used in the temperature response calculations. The calculated interface temperature was 760C from Eqs. 1 and 2 using values of 945C for T_2, 608C for T_1 and a particle bed voidage of 0.86. The initial temperature profile across the base plate was not as uniform as for test FDE-3. The temperature changes at each position were calculated relative to its initial temperature. These are tabulated in Table A3 and plotted on Figs. A2, A3, and A4 in comparison with the data. Again the calculated response at the point 6.35 mm below the surface exceeds that recorded from the thermocouple because of the assumptions of a semi-infinite media and a constant interface temperature. However, the agreement at 12.7 and 19.05 mm below the surface is excellent.

FDE-5

In this experiment with U-10 wt% Fe and a sodium depth of 0.3 m the temperature arrest in TC-19 occurred at 750C. The middle thermocouple at the 12.7 mm position in the steel plate did not indicate because an open circuit developed during the test. There was a large deviation between the initial temperatures of the other two thermocouples. The initial temperature of TC-20, 6.35 mm below the surface, was 608C; whereas TC-22, 19.05 mm below the surface was at 588C. Because of this considerable temperature deviation within the steel plate in addition to the other simplifying assumptions used in the calculations, it was not meaningful to attempt a comparison between experimental and calculated values.

This simple calculational technique, however, does indicate that impingement heat flux is amenable to calculation. Refined calculations with better defined boundary conditions should readily yield more realistic temperature responses.

Table A2.
Calculated Temperature Response of Base Plate for FDE-3

	$x = 6.35 \times 10^{-3}$ m		$x = 1.27 \times 10^{-2}$ m		$x = 1.905 \times 10^{-2}$ m	
t,s	erf $\frac{x}{2\sqrt{\alpha_1 t}}$	T	erf $\frac{x}{2\sqrt{\alpha_1 t}}$	T	erf $\frac{x}{2\sqrt{\alpha_1 t}}$	T
0	1.000	606	1.000	606	1.000	606
1	0.968	611	1.000	606	1.000	606
2	0.870	626	1.000	606	1.000	606
3	0.787	639	0.987	608	1.000	606
4	0.718	649	0.968	611	1.000	606
5	0.664	658	0.946	614	1.000	606
6	0.619	665	0.921	618	0.991	607
7	0.580	671	0.896	622	0.985	608
8	0.555	675	0.870	626	0.977	610
9	0.529	678	0.847	630	0.968	611
10	0.503	683	0.825	633	0.958	612

Table A3.
Calculated Temperature Response of Base Plate for FDE-4

	$x = 6.35 \times 10^{-3}$ m		$x = 1.27 \times 10^{-2}$ m		$x = 1.905 \times 10^{-2}$ m	
t,s	erf $\frac{x}{2\sqrt{\alpha_1 t}}$	T	erf $\frac{x}{2\sqrt{\alpha_1 t}}$	T	erf $\frac{x}{2\sqrt{\alpha_1 t}}$	T
0	1.000	608	1.000	611	1.000	595
1	0.968	613	1.000	611	1.000	595
2	0.870	626	1.000	611	1.000	595
3	0.787	641	0.987	613	1.000	595
4	0.718	652	0.968	616	1.000	595
5	0.664	661	0.946	619	1.000	595
6	0.619	668	0.921	623	0.991	596
7	0.580	674	0.896	627	0.985	598
8	0.555	678	0.870	631	0.977	599
9	0.529	682	0.847	635	0.968	600
10	0.503	686	0.825	638	0.958	602

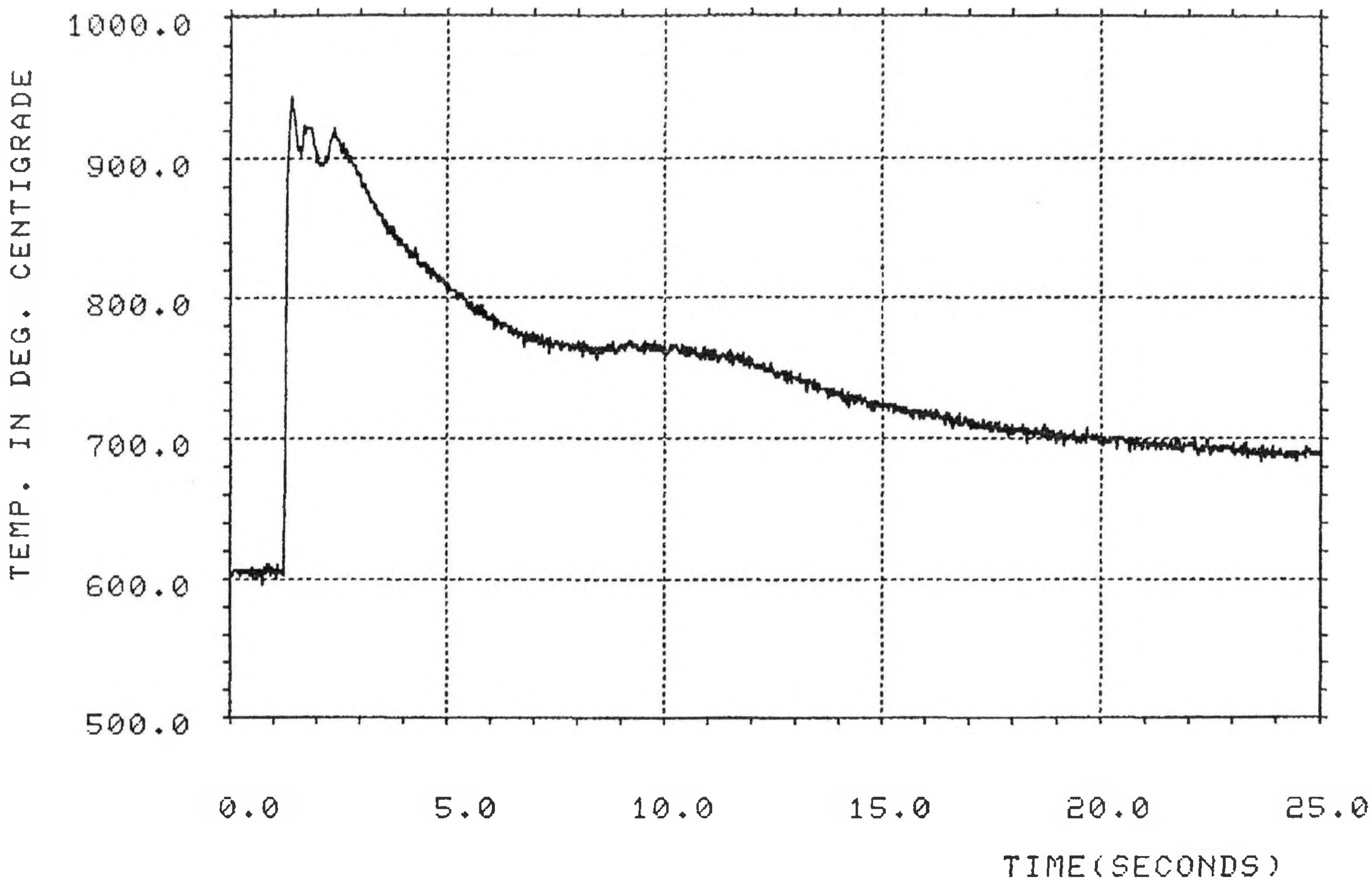

TC-18, FUEL DROP EXPT.#4, DATE 9/25/87

Fig. A1

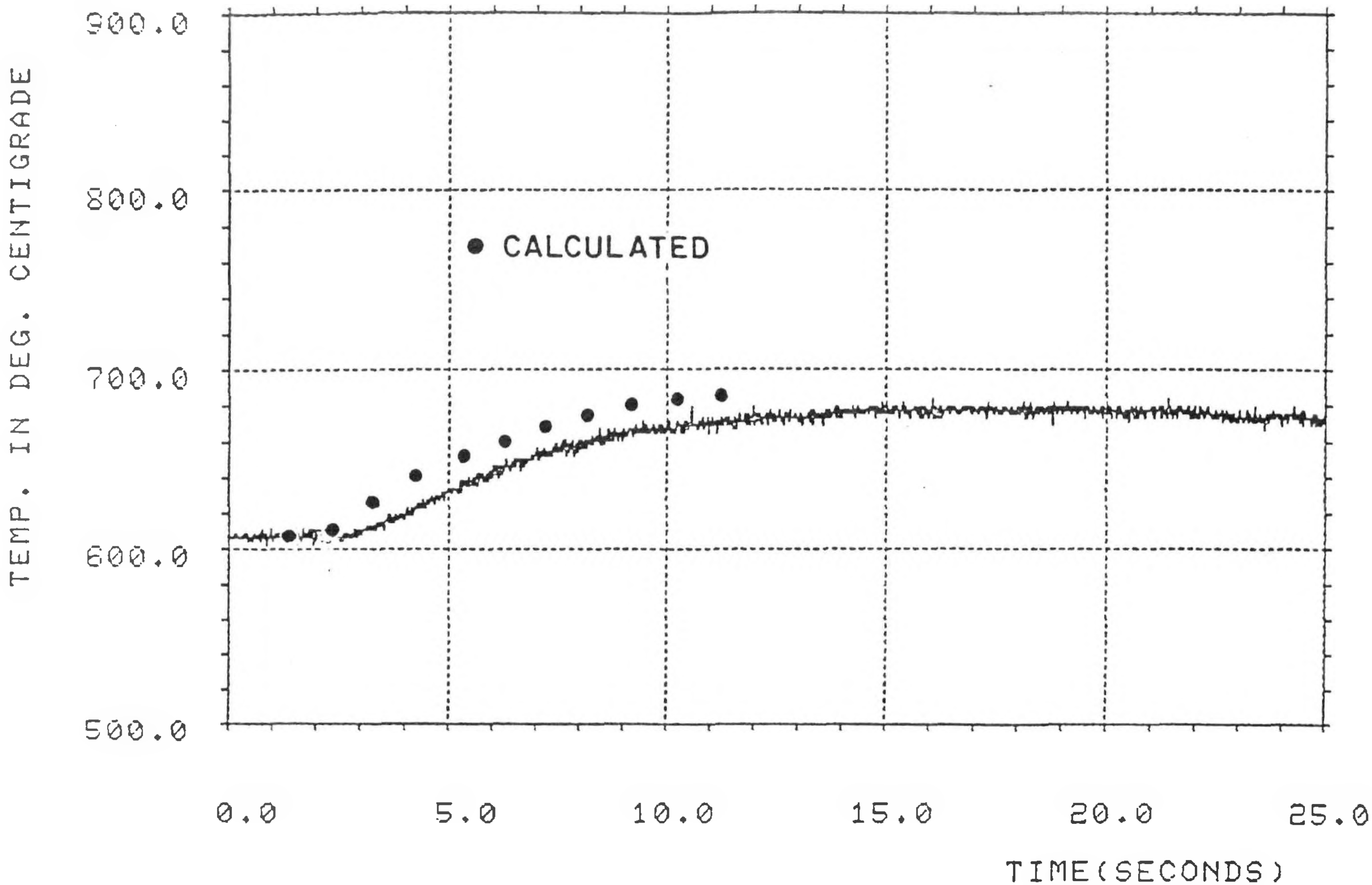

TC-20, FUEL DROP EXPT. #4, DATE 9/25/87

Fig. A2

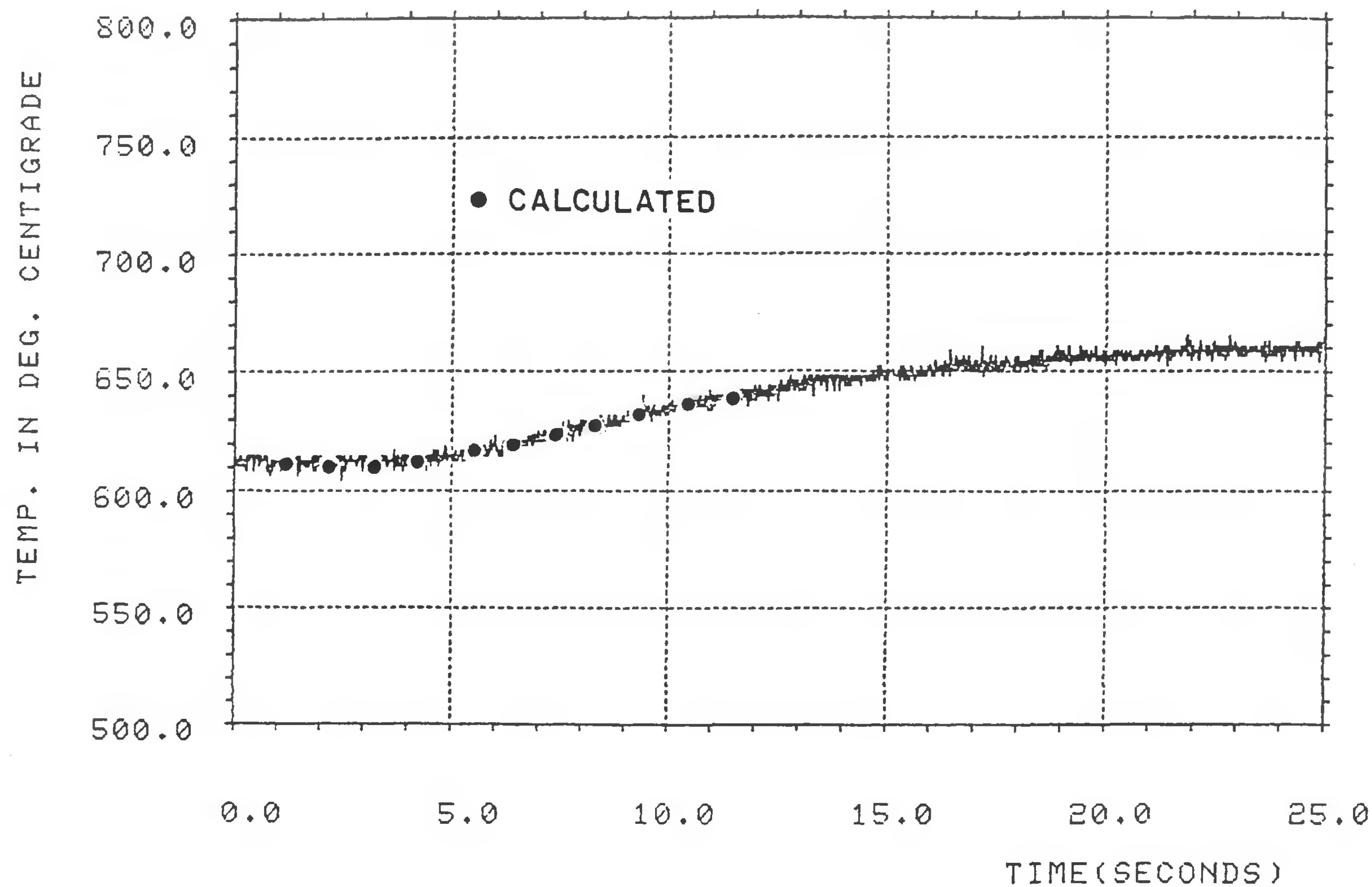

TC-21, FUEL DROP EXPT. #4, DATE 9/25/87

Fig. A3

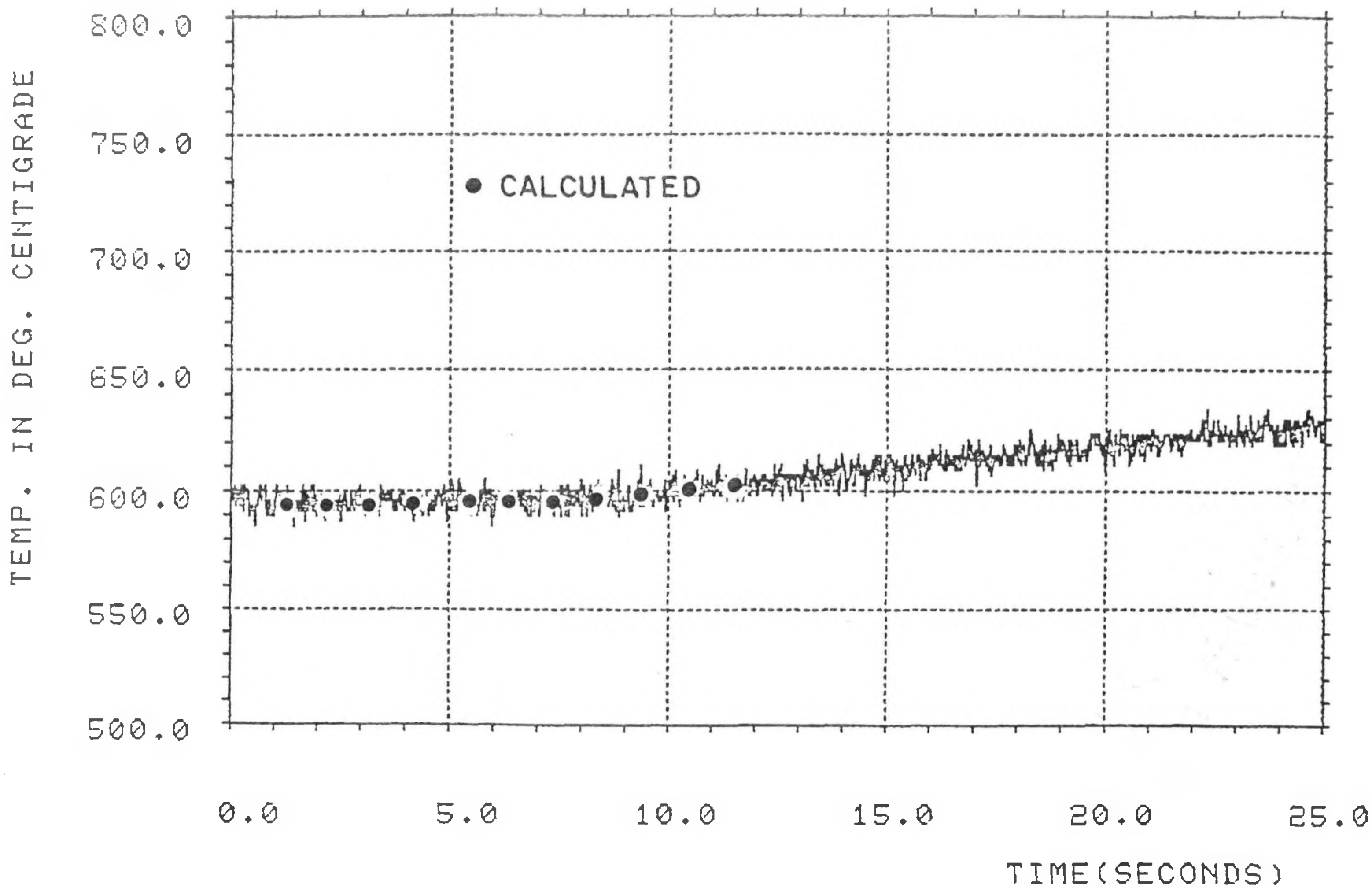

TC-22, FUEL DROP EXPT. #4, DATE 9/25/87

Fig. A4

APPENDIX B

TAYLOR MODEL FOR BREAKUP LENGTH

Taylor[14] developed a semi-empirical model for breakup lengths for turbulent jets. This model was derived from his analysis of the generation of ripples caused by wind blowing over a viscous fluid. The wind was assumed to exert normal pressure on the surface but no tangential (frictional) stress on the free surface. This analysis was then extended by Taylor[15] to the dispersion of larger diameter (~20 mm) liquid-metal jets in water. The length of the jet before breakup in a fluid (system 1) was determined by comparison with existing data for jets and fluid environments with different densities (system 2). The resulting equation is:

$$L_2 = L_1 \left(\frac{\rho_j}{\rho_f}\right)_2^{1/2} \Bigg/ \left(\frac{\rho_j}{\rho_f}\right)_1^{1/2} \qquad \text{(B1)}$$

Taylor used as a basis a breakup length of 150 jet diameters for a water jet in air and five jet diameters for a water jet in water. Application of Eq. B1 to uranium metal in sodium at 600C using water-water as the basis for system 2 gives:

$$L_2 = 5\left(\frac{17.5}{0.808}\right)^{1/2} \Bigg/ \left(\frac{1.0}{1.0}\right)^{1/2} = 23.3$$

For a pour stream diameter of 25 mm the predicted breakup length is 0.58 m.

Epstein and Fauske[13] considered the breakup of jets blanketed by the vapor of the liquid in which they are injected. Epstein and Fauske following the method outlined by Levich[16] obtained for a zero equivalent vapor blanket the following length to diameter ratio:

$$L = \frac{\sqrt{3}}{2}\left(1 + \frac{\rho_\ell}{\rho_j}\right)\left(\frac{\rho_j}{\rho_\ell}\right)^{1/2} \qquad \text{(B2)}$$

Therefore, for the molten uranium-sodium system the length-to-diameter ratio, L, is:

$$L = \frac{\sqrt{3}}{2}\left(1 + \frac{0.808}{17.5}\right)\left(\frac{17.5}{0.808}\right)^{1/2} = 4.22$$

For a pour stream diameter of 25 mm the predicted breakup length is 0.105 m.

APPENDIX C

FDE-1 THERMOCOUPLE RESPONSE

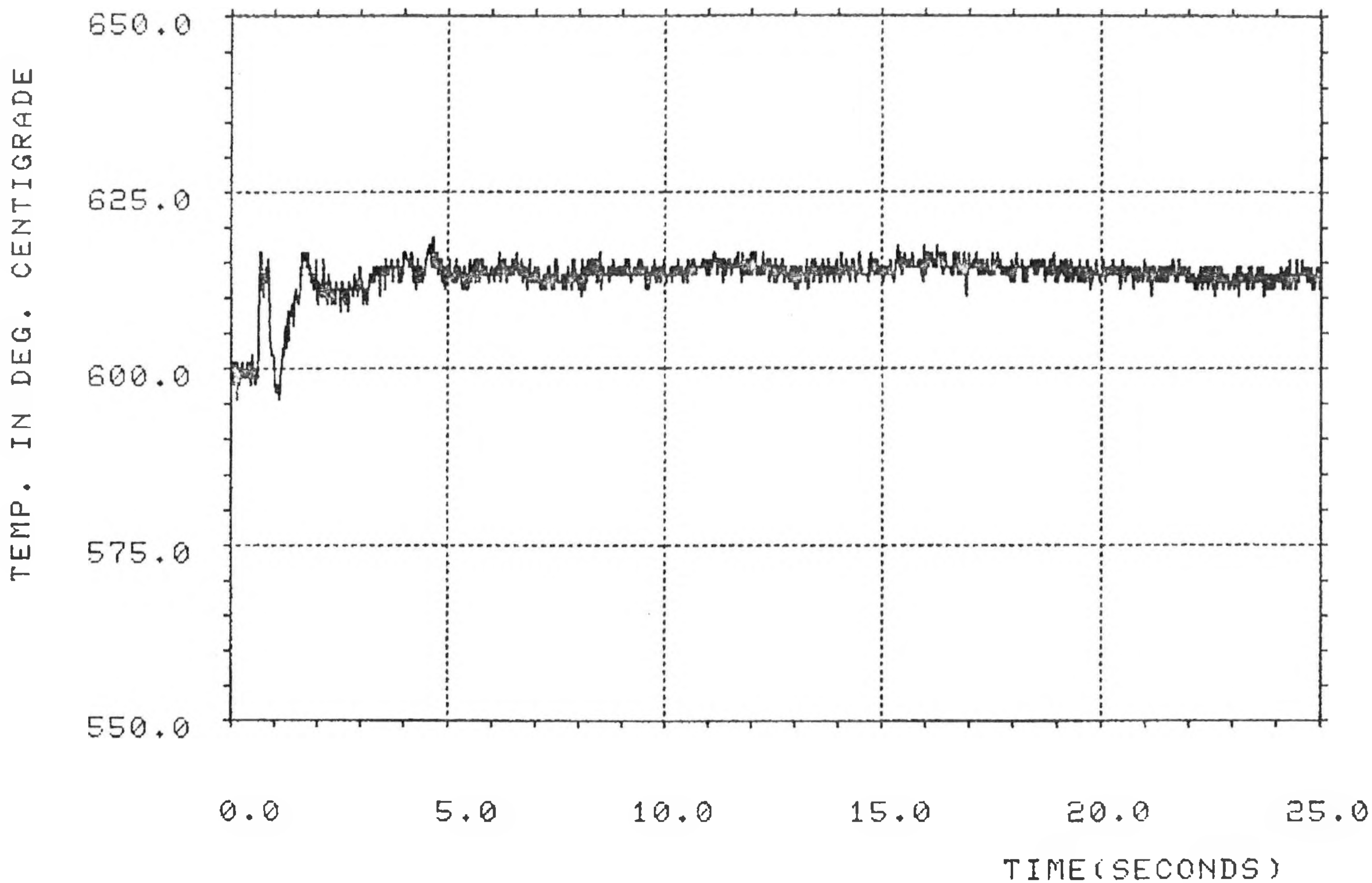

TC-17, FUEL DROP EXPT.#1, DATE 7/22/87

Fig. C1

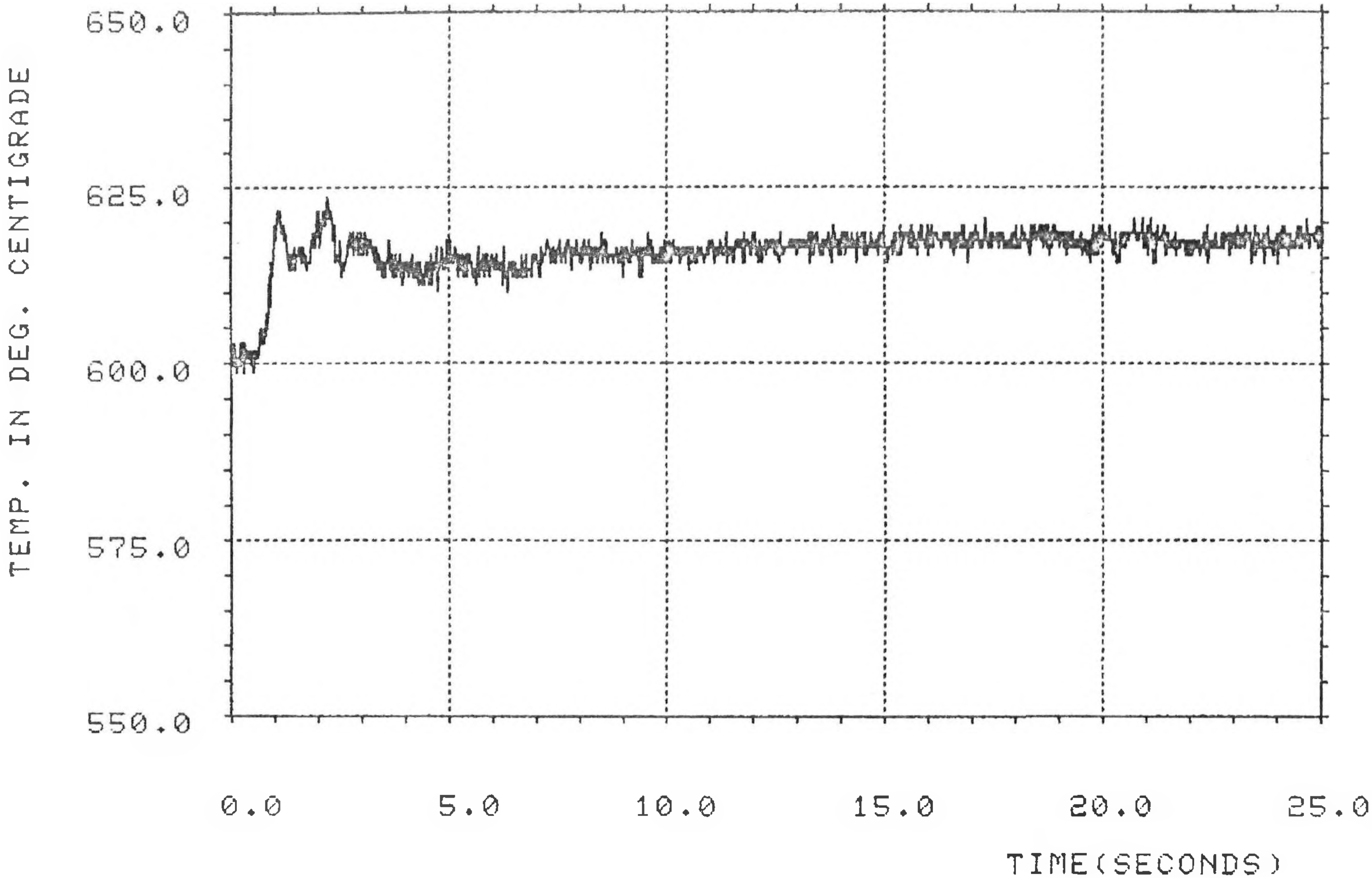

TC-18, FUEL DROP EXPT.#1, DATE 7/22/87

Fig. C2

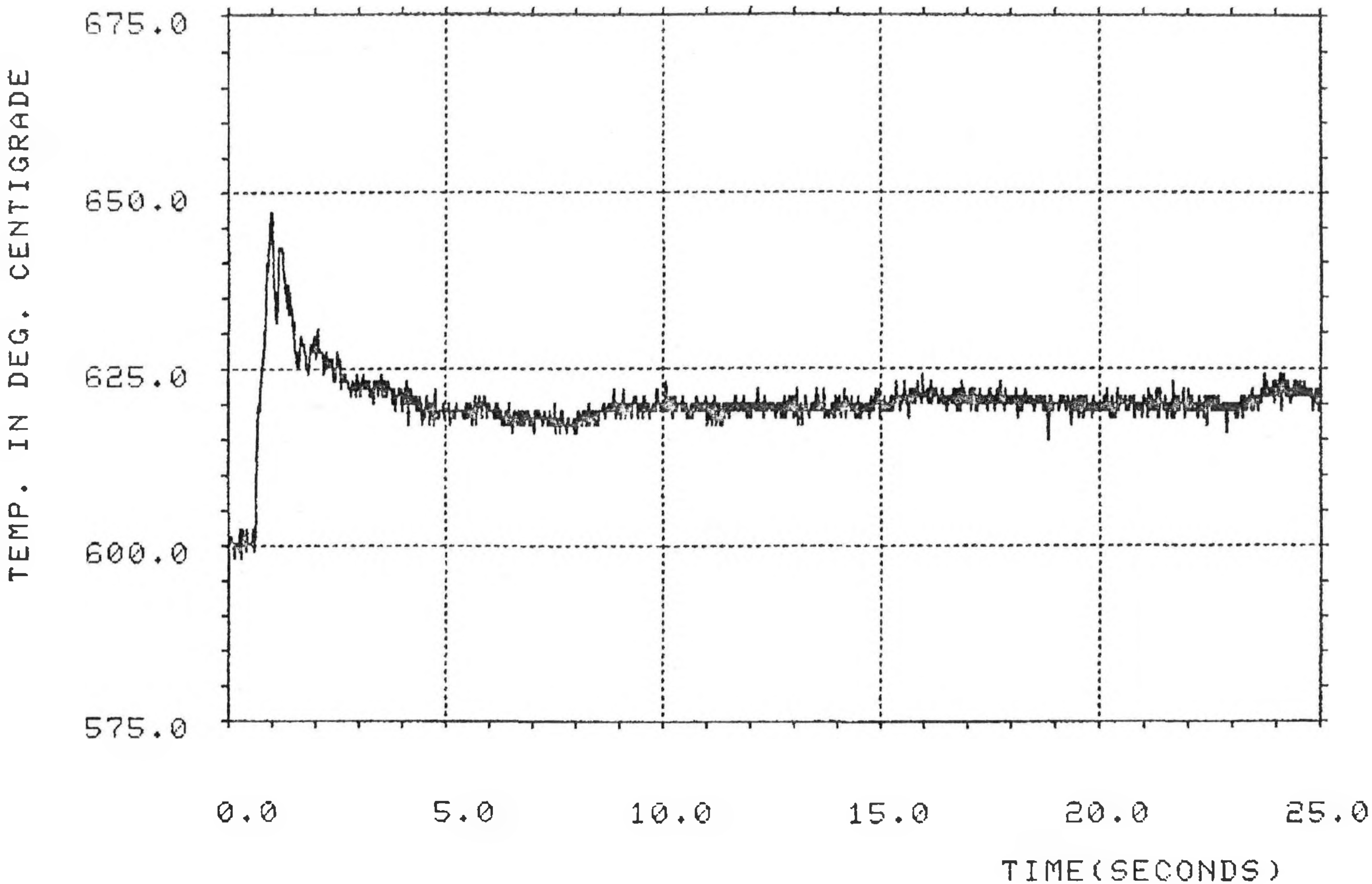

TC-19, FUEL DROP EXPT.#1, DATE 7/22/87

Fig. C3

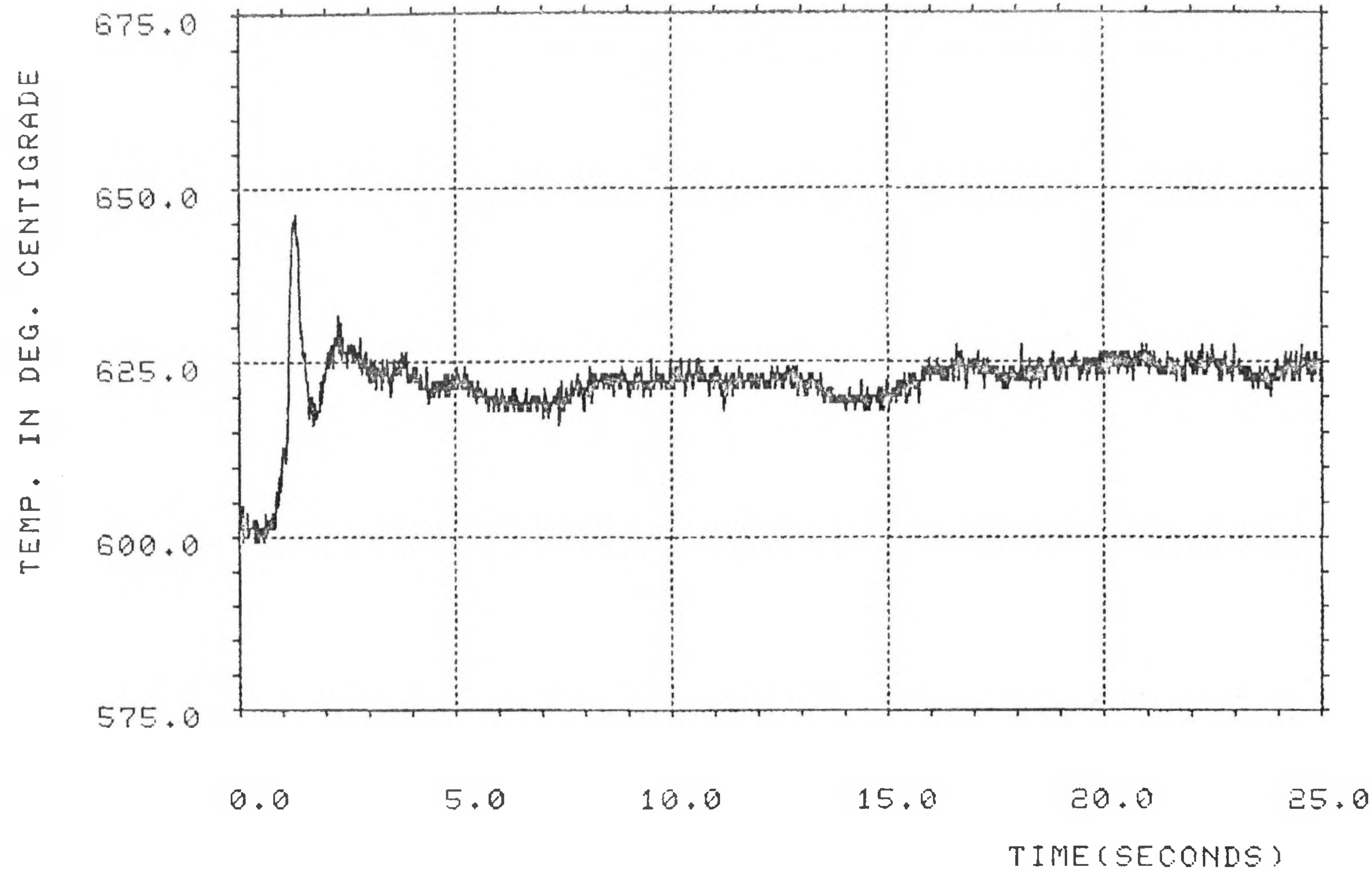

TC-20, FUEL DROP EXPT.#1, DATE 7/22/87

Fig. C4

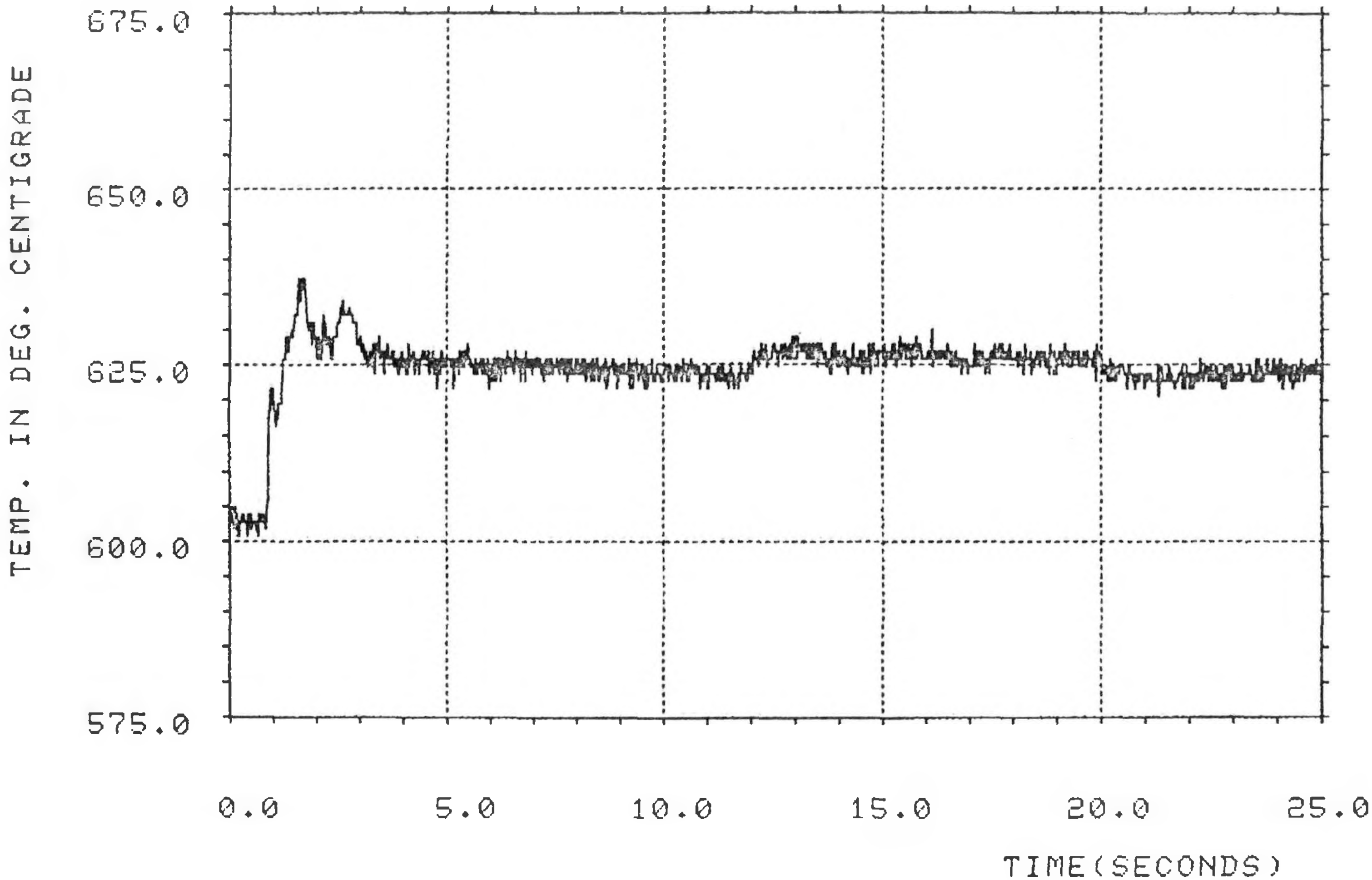

TC-21, FUEL DROP EXPT.#1, DATE 7/22/87

Fig. C5

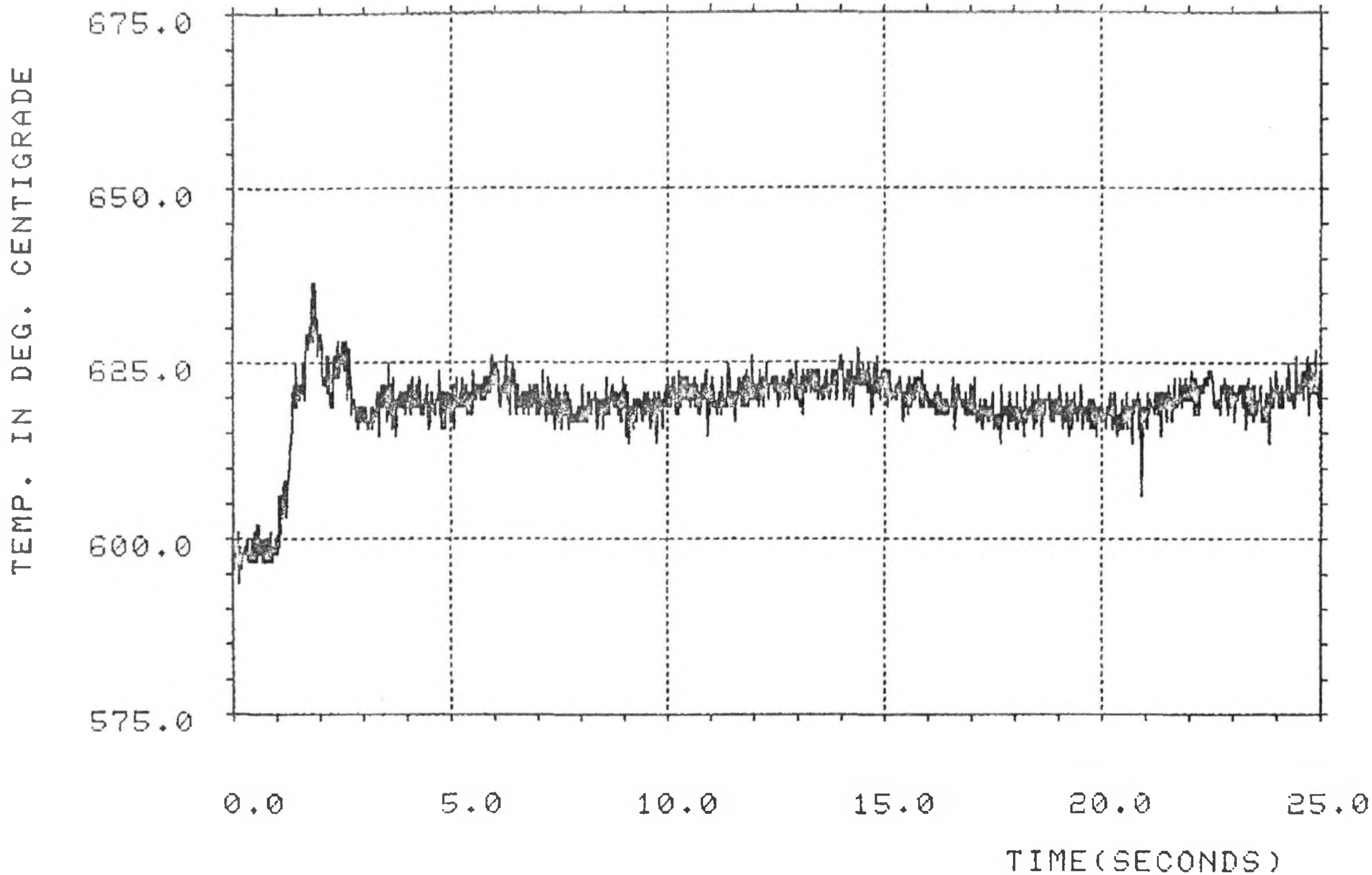

TC-22, FUEL DROP EXPT.#1, DATE 7/22/87

Fig. C6

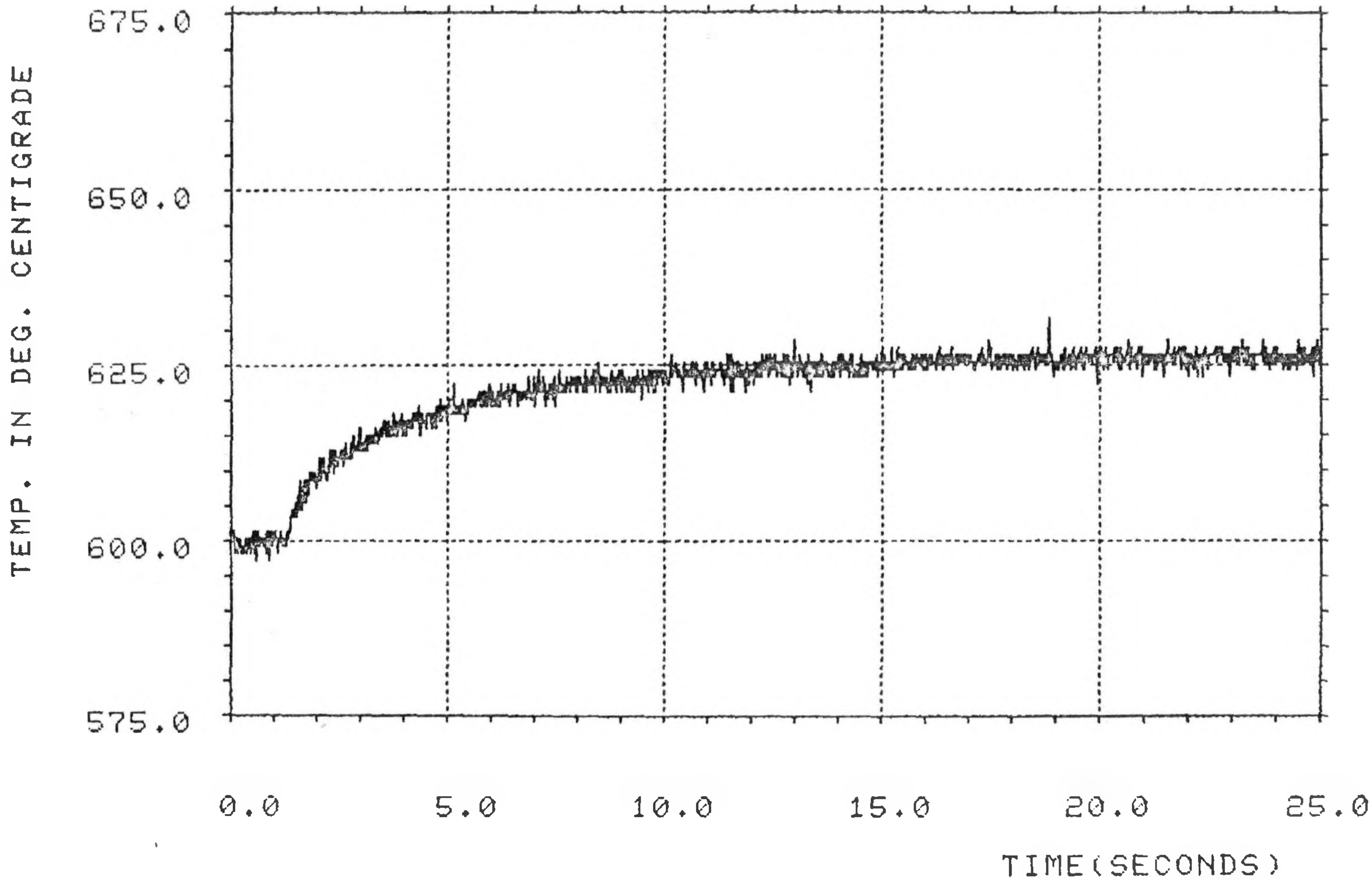

TC-23, FUEL DROP EXPT.#1, DATE 7/22/87

Fig. C7

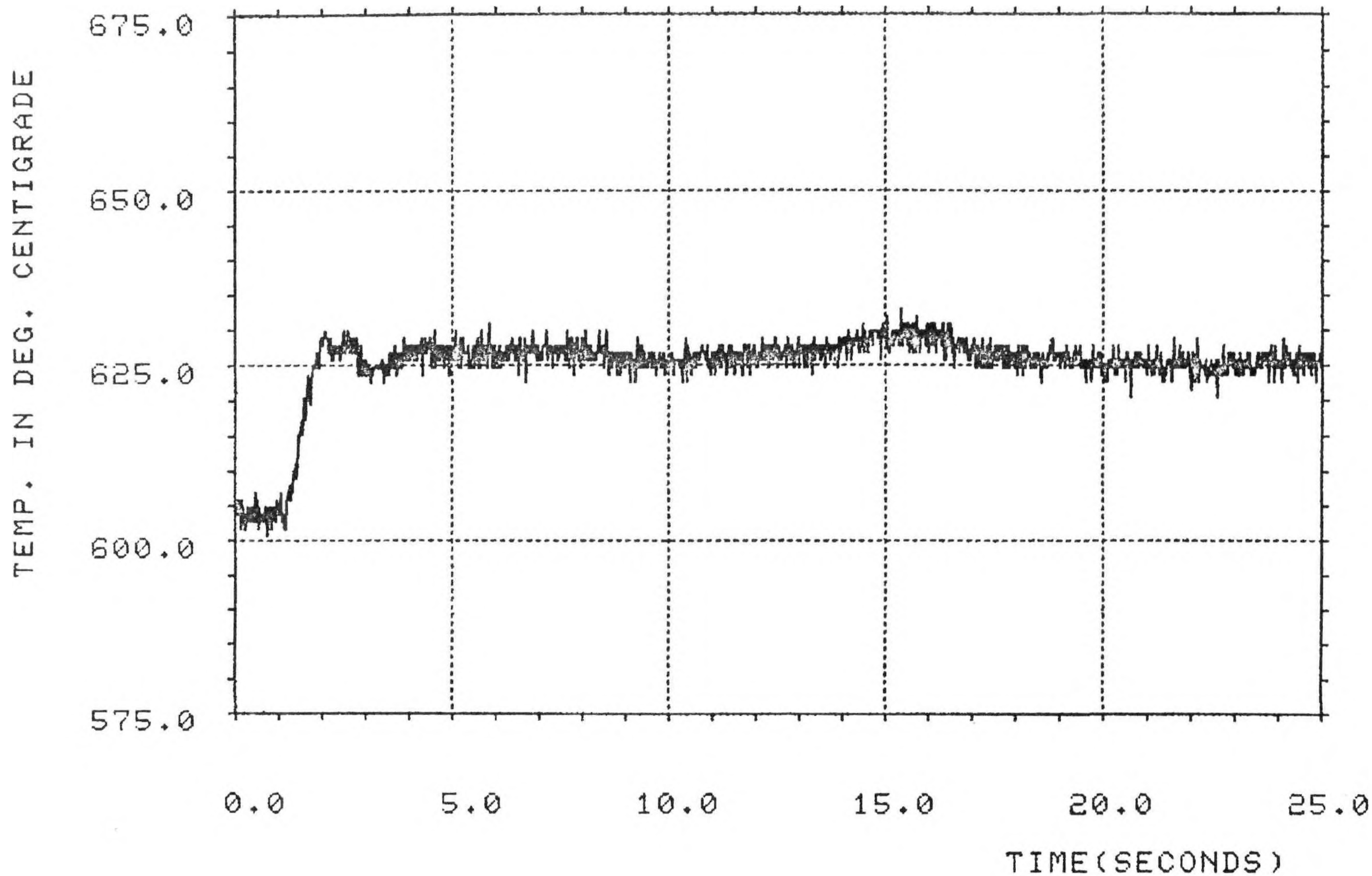

TC-24, FUEL DROP EXPT.#1, DATE 7/22/87

Fig. C8